REVIEW ARTICLE

High power ultrafast lasers

Sterling Backus, Charles G. Durfee III, Margaret M. Murnane,[a] and Henry C. Kapteyn
Center for Ultrafast Optical Science, University of Michigan, Ann Arbor, Michigan 48109-2099

(Received 25 March 1997; accepted for publication 2 December 1997)

In this article, we review progress in the development of high peak-power ultrafast lasers, and discuss in detail the design issues which determine the performance of these systems. Presently, lasers capable of generating terawatt peak powers with unprecedented short pulse duration can now be built on a single optical table in a small-scale laboratory, while large-scale lasers can generate peak power of over a petawatt. This progress is made possible by the use of the chirped-pulse amplification technique, combined with the use of broad-bandwidth laser materials such as Ti:sapphire, and the development of techniques for generating and propagating very short (10–30 fs) duration light pulses. We also briefly summarize some of the new scientific advances made possible by this technology, such as the generation of coherent femtosecond x-ray pulses, and the generation of MeV-energy electron beams and high-energy ions. © *1998 American Institute of Physics.* [S0034-6748(98)00303-7]

I. INTRODUCTION

Ultrafast optical science is a field of diverse applications with two common themes: the use of ultrashort (10^{-12}–10^{-14} s) light pulses to elucidate fast-evolving events in materials and chemical systems, and the use of these pulses to concentrate an extremely high-energy density into a small volume. The 1990s have seen a revolution in ultrafast laser technology.[1–4] Ultrafast light sources today are ''turnkey'' devices, producing peak output powers on the order of a megawatt in a pulse duration of under 10 fs, directly from a simple laser.[5–8] Since the optical cycle period in the visible and near infrared is 2–3 fs, this pulse duration is nearing the physical limits of devices operating in this wavelength range.

For many experiments, however, a peak power of a megawatt is not sufficient, making it necessary to increase the energy of these short pulses using a laser amplifier system. The technology for generating high-power amplified ultrafast pulses has also progressed rapidly over the past decade.[9–17] Amplification of the energy in an ultrashort pulse by factors of 10^6 or more is now routinely achieved, resulting in a peak power of $>10^{12}$ W (terawatts, or TW) from small-scale lasers, or $\sim 10^{15}$ W (petawatts) from larger systems.[18] By focusing these high power optical pulses, light intensities of greater than 10^{20} W cm^{-2} can be generated—an intensity greater than that which would be obtained by focusing the entire solar flux incident on the earth, onto a pinhead. Because the size of a laser depends primarily on its pulse energy, it is only by reducing the duration of a pulse that we can achieve extremely high power densities using lasers of a realistic scale. Progress in laser amplifier systems has made it possible to generate pulses at high powers which are nearly as short ($\sim$20 fs) as can be generated at low energy. As a result, even very small-scale laboratory lasers operating at kilohertz repetition rates are now capable of generating light intensities corresponding to an electric field easily in excess of that binding a valence electron to the core of an atom.[16,19]

Remarkable progress in high-field optical science has followed as a direct result of these recent technological advances. It is now possible to experimentally investigate highly nonlinear processes in atomic, molecular, plasma, and solid-state physics, and to access previously unexplored states of matter.[20–31] Coherent ultrashort pulses at ultraviolet and soft x-ray wavelengths down in 2.7 nm can be generated through harmonic upconversion,[20,22–24,26,32,33] and also at hard and soft x-ray wavelengths through the creation of an ultrafast laser-produced plasma.[21] Such ultrafast soft- and hard-x-ray pulses can be used to directly probe both long- and short-range atomic dynamics, and to monitor the evolution of highly excited systems.[34] In the future, these coherent x-ray sources may be used for x-ray microscopy, lithography, and metrology. These high peak-power ultrashort pulses can also be further compressed to sub-10 fs duration at millijoule energy through the use of self-phase modulation in hollow-core waveguides and pulse compression.[35–37] New guided-wave techniques for efficient phase-matched frequency upconversion now make it possible to extend ultrafast techniques into the ultraviolet and the vacuum-ultraviolet regions of the spectrum with $\sim$10 fs time resolution.[38]

In other work, the use of extremely short-pulse high-intensity lasers may make it possible to generate coherent x-rays with pulse durations as short as 10^{-16} s (100 attoseconds). This work exploits a new regime in laser–atom inter-

[a]Electronic mail: murnane@umich.edu

actions, making it possible to use precisely ''shaped'' light pulses to manipulate atoms and optimize the x-ray generation process.[31,39,40] The required fractional bandwidth to support an ultrashort pulse is less at shorter wavelengths: to support a 1 fs pulse with a center wavelength of 800 nm, a full width at half-maximum (FWHM) bandwidth of $\Delta\lambda \approx \lambda$ is required. In contrast, to support the same 1 fs pulse at a wavelength of 10 nm, the required FWHM bandwidth drops to only 0.1 nm. The generation of subfemtosecond pulses may be achieved in the near future using either high-order harmonic generation,[31,39] or using the interaction of an intense ionizing pulse with a gas.[41]

At intensities much higher than required to ionize an atom, other phenomena become observable. These intensities are accessible using terawatt- or multiterawatt-scale lasers. For example, several novel relativistic nonlinear optical effects occur when a free electron oscillates in the laser field at nearly the speed of light, because its relativistic mass ($m = \gamma m_0$) then exceeds its rest mass (m_0). These include the generation of wakefield-plasma-waves,[42] self-focusing,[43] electron cavitation, nonlinear Thomson scattering, electron–positron pair production, ultrarelativistic interactions, and gigagauss magnetic fields. At these high peak powers, the direct acceleration of electrons by laser beams can occur.[42] For example, recent work has demonstrated that by using an intense laser pulse focused into a gas a collimated electron beam with an energy >10 MeV can be generated.[29,30] This new method of electron acceleration is exciting not only for high-energy physics, but also for more immediate applications such as materials processing, the generation of x rays for time-resolved x-ray diffraction, and as an improved electron source for future generation conventional accelerators. Other work will use ultrashort-pulse, ultrahigh-peak-power lasers to implement new types of x-ray lasers operating at wavelengths much shorter than available to date.[44,45] All currently demonstrated schemes have limited prospects for generating coherent light at wavelengths much shorter than 5 nm.[46] However, the use of high-power, ultrafast lasers will make it feasible to implement a new class of x-ray excited,[47,48] or recombination-pumped[49] lasers which may operate at wavelengths as short as 1.5 nm (850 eV photon energy). Still other work showed that Compton scattering of an intense laser from a relativistic electron beam (generated from a linac) can produce hard x rays at 5 keV energies.[50] Finally, ultrashort-pulse, high-power lasers will be used to test the ''fast ignitor'' concept in inertial-confinement fusion (ICF) physics, where a preheated core of nuclear material will be rapidly heated to initiate fusion using a short, intense light pulse.[51] Thus, from a fundamental and practical point of view, high-power, ultrafast lasers show great promise for future applications.

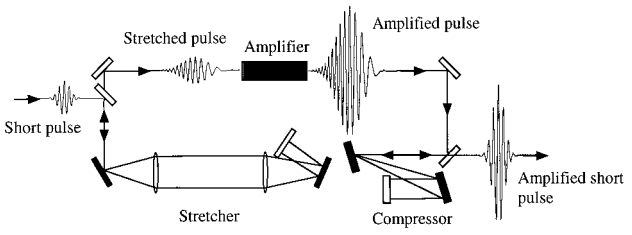

FIG. 1. Schematic diagram of an amplifier system based on chirped-pulse amplification.

II. ENABLING DEVELOPMENTS FOR HIGH PEAK-POWER LASER SYSTEMS

A. Chirped-pulse amplification

Nearly all high peak-power, ultrafast laser systems make use of the technique chirped-pulse amplification (CPA), followed by optical pulse compression, as illustrated in Fig. 1. The application of CPA to lasers originated with the work of Mourou and his co-workers;[9,10,52,53] previous to this, CPA had been used in microwave (radar) applications. The concept behind CPA is a scheme to increase the energy of a short pulse, while avoiding very high peak powers in the laser amplification process itself. This is done by lengthening the duration of the pulse being amplified, by dispersing, or ''chirping'' it in a reversible fashion, using the technique of optical pulse compression, developed by Treacy and Martinez.[54–58] By lengthening the pulse in time, energy can be efficiently extracted from the laser gain medium, while avoiding damage to the optical amplifier. CPA is particularly useful for efficient utilization of solid-state laser media with high stored energy density ($1-10$ J/cm^2), where full energy extraction in a short pulse would lead to intensities above the damage threshold of the amplifier materials.

The CPA scheme works as follows (see Fig. 1). (1) Ultrashort light pulses are generated at low pulse energy through the use of an ultrashort-pulse modelocked laser ''oscillator.'' This modelocked laser typically generates light pulses at a high repetition rate ($\approx 10^8$ Hz) with pulse energies in the range of 10^{-9} J, and with pulse durations in the range of $10^{-12}-10^{-14}$ s. (2) These femtosecond pulses are then chirped using a dispersive delay line consisting of either an optical fiber or a diffraction-grating arrangement. The pulse is stretched from a duration under 100 fs to typically ~ 100 ps, decreasing its peak power by approximately three orders of magnitude. (3) One or more stages of laser amplification are used to increase the energy of the pulse by six to nine orders of magnitude to a fluence sufficient to efficiently extract energy from the laser amplifiers. This amplification typically requires a total of between 4 and 50 passes through an amplification medium, with a gain of between 2 and 100 per pass. (4) After optical amplification, when the pulse is very energetic, a second grating pair is then used to ''recompress'' the pulse back to femtosecond duration. To achieve this recompression back to near the original input pulse duration, proper optical design of the amplifier system is very important.

B. Ultrashort-pulse laser oscillators

The CPA scheme separates the ultrashort-pulse generation process from the amplification process. Although the first CPA laser system was demonstrated in 1986,[9] CPA was not widely used until after the development of simple and reliable modelocked femtosecond laser sources operating in the wavelength range of broad-bandwidth solid-state laser materials such as Ti:sapphire (800 nm), Nd:glass (1.06 μm),

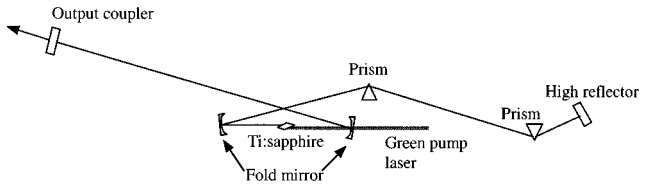

FIG. 2. Schematic diagram of a self-modelocked Ti:sapphire laser.

and Cr:LiSAF (850 nm).[1,3] Prior to 1990, most CPA work was done using either modelocked Nd:YAG oscillators at 1.06 μm, or synchronously pumped modelocked dye lasers at wavelengths around 800 nm.[10,52,53,59,60] However, both of these types of lasers were extremely sensitive to environmental perturbations, and thus unstable and difficult to use. Moreover, since Nd:YAG lasers typically generate pulses of 10–100 ps, nonlinear self-phase modulation techniques[61] were required to broaden the bandwidth of these pulses, resulting in recompressed pulse durations of approximately 1 ps. An alternative means of generating ultrashort pulses at 800 nm was to use a colliding-pulse modelocked (CPM) laser operating at 620 nm,[62] amplify the pulse in dye amplifiers, and then to use self-phase modulation or parametric generation[63] to convert a small fraction of this pulse energy into light at 800 nm. The difficulties inherent in all of these methods made progress in the design of the amplifier systems difficult, laborious, expensive, and most important, frustrating to those working on the technology.

The situation changed dramatically, however, with the demonstration of the self-modelocked Ti:sapphire laser by Sibbet and his group in 1990.[1] Titanium-doped sapphire is a solid-state laser material with extremely desirable properties: a gain bandwidth spanning the wavelength region from 700 to 1100 nm, very high thermal conductivity, and an energy storage density approaching 1 J/cm^2. This last property, although desirable for high-energy amplification, was thought to prohibit the use of Ti:sapphire in femtosecond modelocked lasers. Existing passively modelocked dye lasers relied on the low-energy storage density of the laser dye to facilitate the modelocking process,[64] and thus passive modelocking is not feasible using most solid-state gain media. However, the self-modelocked Ti:sapphire laser relies on a different mechanism to facilitate short-pulse generation—the Kerr nonlinearity of the laser crystal. Since this nonlinearity is instantaneous and independent of the energy storage density of the laser medium, it made possible an entirely new class of reliable, high average power, ultrashort-pulse ($<$10 fs) lasers.[5–7,65]

Although self-modelocking has been used to generate ultrashort pulses in a number of different laser media, by far the most common such laser is still the Ti:sapphire laser. The basic cavity configuration is quite simple, as shown in Fig. 2. The energy source for the laser is a continuous wave (cw) laser—typically an argon-ion laser. More recently, commercially available cw diode-pumped frequency-doubled YAG lasers have also found widespread application.[66] The cw light is focused into the Ti:sapphire crystal, collinear with the mode of the laser cavity itself. The only other cavity components are an end mirror and an output coupler, together with a prism pair to compensate for dispersion of the Ti:sapphire crystal.[67] Modelocking in this laser is achieved through the action of the Kerr lens induced in the laser crystal itself. If the laser is operating in a pulsed mode, the focused intensity inside the Ti:sapphire crystal exceeds 10^{11} W/cm^2—sufficient to induce a strong nonlinear lens which quite significantly focuses the pulse. If this occurs in a laser cavity which is adjusted for optimum efficiency without this lens, this self-focusing will simply contribute to loss within the laser cavity. However, modest displacement of one mirror away from the optimum cw position by only 0.5–1 mm can result in a decrease in loss in the laser cavity when Kerr lensing is present. Thus, the Kerr lensing couples the spatial and temporal modes of the oscillator, resulting in two distinct spatial and temporal modes of operation (cw and pulsed).[68] The laser can be simply aligned to be stable in either mode.

The most significant advance in Ti:sapphire oscillator design since its original demonstration has been a dramatic reduction in achievable pulse duration. This was accomplished by reducing overall dispersion in the laser by using physically shorter Ti:sapphire crystals and optimum prism materials or mirrors.[5–7,65,69,70] It is now routine to generate pulse durations of 10 fs directly from such a laser at a repetition rate of $\approx$80 MHz, with pulse energy of approximately 5–10 nJ, and with excellent stability. Such a laser is an ideal front-end source for a high-power, ultrafast, amplifier system.

The laser configuration of Fig. 2 can generate pulses as short as $\sim$8 fs duration.[6] At these short durations, the spectral shape of the pulses from the laser is no longer a simple Gaussian or sech^2 shape, but is modulated by higher-order dispersion originating from the prism dispersion compensation. This spectrum shape and center wavelength can be adjusted to obtain shorter pulses out of the laser amplifier than might otherwise be expected, as will be discussed. Somewhat shorter pulse durations ($\sim$7 fs) can be obtained from a Ti:sapphire laser by using mirror dispersion compensation[71] instead of or as well as prism compensation.[72] Difficulties in the use of dispersion-compensating mirrors include stringent manufacturing tolerances which result in varying performance and a lack of continuous adjustability of the net cavity dispersion.

The ultimate limits of pulse duration from the modelocked Ti:sapphire laser are still a subject of investigation. The coupling of spatial and temporal modes in the laser becomes complex at very short pulse durations; for example, the divergence of different spectral components of the pulse varies considerably over the bandwidth of even a $\sim$10 fs pulse.[73–75] Nevertheless, it is likely that further improvements in dispersion compensation techniques and broad-bandwidth low-loss mirrors will result in pulses at least as short as 5 fs.[76,77] The translation of these developments into improvements in pulse duration from high-power laser amplifiers would await more effective techniques for avoiding gain narrowing in the laser amplifiers.[78]

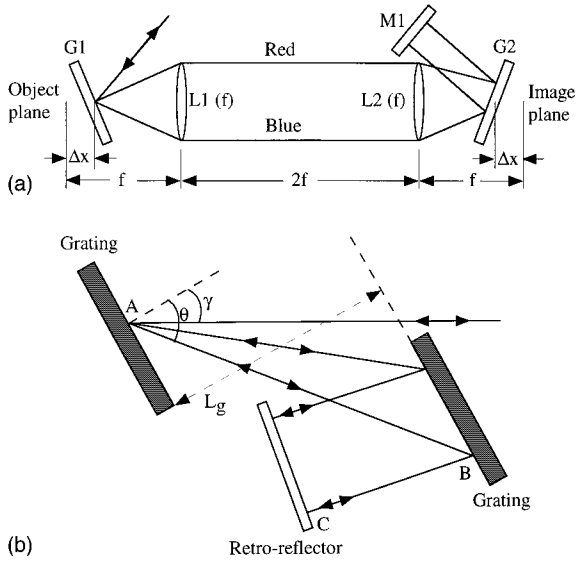

FIG. 3. Schematic diagrams of (a) a pulse stretcher and (b) a pulse compressor.

III. DESIGN OF HIGH PEAK-POWER LASER SYSTEMS

Typically, several design choices must be made in developing a high-power ultrafast laser system, involving trade-offs between pulse energy, pulse duration, spatial quality, pulse contrast, repetition rate, and wavelength. Nevertheless, as discussed above, and as illustrated in Fig. 1, most systems have many features in common—a front-end laser, a pulse stretcher, several stages of amplification, and a pulse compressor. In the following sections we discuss in detail the various components of a high-power ultrafast laser system. We also mention some specialized systems which are optimized for particular applications.

A. Pulse stretching and recompression

Before injection into the amplifier, the short pulse (10 fs–1 ps) is stretched in time by introducing a frequency chirp onto the pulse, which increases the duration by a factor of 10^3-10^4 (to $\approx$100 ps). The duration of the stretched pulse is determined by the need to avoid damage to the optics and to avoid nonlinear distortion to the spatial and temporal profile of the beam. A frequency-chirped pulse can be obtained simply by propagating a short pulse through optical material, such as a fiber. In the fiber, self-phase modulation (SPM) can broaden the bandwidth of the pulse; however the distortion due to high-order phase terms introduced by fibers make it difficult to use this design for femtosecond pulses. To obtain even even greater stretch factors, a grating or prism pair arrangement can be used which separates the spectrum of a short pulse in such a way that different colors follow different paths through the optical system. Martinez realized that by placing a telescope between a grating pair, as shown in Fig. 3(a), the dispersion is controlled by the effective distance between the second grating and the image of the first grating.[57,58] When this distance is optically made to be negative, the arrangement has exactly the opposite dispersion of a grating compressor, shown in Fig. 3(b). This forms the basis for a perfectly matched stretcher/compressor pair. Stretching and recompression with gratings thus allows large, reversible stretch factors. Any imperfections in the recompression result largely from the mismatch between the stretcher and compressor separation and incident angles that is required to compensate for the amplifier material and optics also present in the system (see below).

In 1969, Treacy showed that a pair of identical parallel gratings exhibits negative group delay dispersion, and can therefore be used to compensate the chirp imposed by materials.[54] It is straightforward to see that the transit time of a pulse through the grating pair arrangement is longer for shorter wavelengths than for longer wavelengths. The optical path P along ABC, from Fig. 3(b), is

$$P=(L_g/\cos\ \theta)[1+\cos(\gamma-\theta)], \tag{1}$$

where the variables are defined as shown in Fig. 3. The diffracted angle is calculated from the grating equation

$$\sin\ \gamma+\sin\ \theta=\lambda/d, \tag{2}$$

where d is the groove spacing. The group delay τ is given by $\tau=P/c$. Since the diffracted angle θ is larger for longer wavelengths, a transform-limited pulse will emerge negatively chirped (short wavelengths precede longer wavelengths). The phase of the grating compressor can be derived in a number of ways owing to the arbitrary choice in absolute phase and group delay (transit time). The most compact expression is given by Martinez *et al.*[55]

$$\phi_g(\omega)=\frac{2\omega L_g}{c}\left[1-\left(\frac{2\pi c}{\omega d}-\sin\ \gamma\right)^2\right]^{1/2}. \tag{3}$$

The expression given here is for a single pass through the compressor. To avoid the wavelength-dependent walkoff (spatial chirp), a mirror is placed to direct the beam through a second pass. For a sufficiently small beam size, this mirror may be aligned angularly away from retroreflection without causing an unacceptable amount of spatial chirp, but for larger beams, a pair of mirrors is used in a roof geometry to direct the output above and parallel to the input beam. The parallelism of the grating faces and grooves must be carefully aligned to avoid spatial chirp on the output beam. For good output beam quality and focusing, the grating surfaces must also have high optical flatness ($\lambda/4-\lambda/10$).

Using either two gratings in an antiparallel configuration, separated by an even number of lenses, or two gratings in a parallel configuration separated by an odd number of lenses, Martinez demonstrated that large positive dispersions, and therefore large stretch factors, could be obtained.[56–58] In fact, neglecting aberrations in the telescope used to project the image of the first grating, the stretcher phase function is exactly the opposite sign of the compressor [Eq. (3)]. In the original stretcher design, two identical lenses (focal length f) are separated by $2f$, with a pair of antiparallel gratings placed each the same distance s_1 from the nearest lens, as shown in Fig. 3(a). The effective grating separation is then $-2(f-s_1)$. As in the compressor, a retroreflection mirror is used to pass the beam back through the stretcher, with either an angular or lateral deviation for output coupling. An all-reflective stretcher design[14,19] avoids the chromatic aberrations (and expense) of the lenses. Even

better, folded, single grating designs, with a single parabolic or spherical mirror and two flat mirrors,[14] or using two concentric mirrors in an Offner triplet,[79,80] offer important advantages over the two grating designs. They work near-Littrow incident angle (given by $\sin\gamma_{\text{Littrow}}=\lambda/2d$), and maintain alignment while the separation and/or angle of the grating are adjusted. This allows the stretcher to be optimized and also the output chirp of the amplifier to be varied without misaligning the entire amplifier system. Moreover, with a single-grating design, there are no possibilities of antiparallelism or angle mismatch between the gratings, which would distort the output pulse by introducing temporal and spatial chirps that cannot be eliminated in the pulse compressor. Finally, in some stretcher designs the aberrations in the stretcher are designed to provide a beneficial effect in the overall phase compensation of the system.[81]

The action of the entire amplifier system may be best understood in the spectral domain. [The two exceptions to this are (1) self-phase modulation, in which a time-dependent phase is imposed on the pulse resulting from the dependence of the index of refraction on the intensity, and (2) gain saturation in the amplifier medium, in which the leading edge of the pulse extracts more energy than the trailing edge.] Consider the propagation of an input pulse, with amplitude and phase given by

$$E(t)=\xi(t)e^{i[\omega_0 t+\varphi(t)]}, \tag{4}$$

through an optical system. Here, $\xi(t)$ is the slowly varying envelope, ω_0 is the central carrier frequency, while $\varphi(t)$ is the phase deviation from transform limit (the temporal phase). In the case of a Gaussian-shaped pulse, for example, we have

$$E(t)=\xi_0 e^{-(t^2/\tau^2)}e^{i\omega_0 t}, \tag{5}$$

where here $\phi(t)=0$. The Fourier transform of Eq. (5) gives us the corresponding amplitude and phase of the input pulse in frequency space,

$$G(\omega)=\int_{-\infty}^{\infty}E(t)e^{-i\omega t}dt=g(\omega)e^{i\eta(\omega)}, \tag{6}$$

where $g(\omega)$ and $\eta(\omega)$ are the spectral amplitude and phase, respectively. This is a more convenient form to use for the discussion of pulse stretching and recompression, since the output of the system is then simply

$$G'(\omega)=G(\omega)S(\omega)=g(\omega)s(\omega)e^{i[\eta(\omega)+\sigma(\omega)]}, \tag{7}$$

where the complex transfer function of the system $[S(\omega)]$ includes the spectral phase contribution due to the stretcher, compressor, material, and all other amplifier components, $\sigma(\omega)$, as well as any frequency dependent attenuation, $s(\omega)$ (for example, the variable diffraction efficiency of the gratings). After the contribution from each of the elements is included, the output pulse $E'(t)$ is obtained by taking the inverse Fourier transform of $G'(\omega)$

$$E'(t)=\frac{1}{2\pi}\int_{-\infty}^{\infty}G'(\omega)e^{i\omega t}d\omega. \tag{8}$$

To properly model the system, it is most accurate to include the entire spectral phase function for each of the components. Often however, only the first orders of a Taylor expansion of the spectral phase about the central frequency ω_0 are needed

$$\phi(\omega)=\phi(\omega_0)+\phi'(\omega_0)(\omega-\omega_0)+\frac{1}{2}\phi''(\omega_0)(\omega-\omega_0)^2+\frac{1}{6}\phi'''(\omega_0)(\omega-\omega_0)^3+\ldots\ldots, \tag{9}$$

where φ', φ'', and φ''' are the derivatives of the phase with respect to frequency, and are known, respectively, as the group delay, second-order dispersion [or group velocity dispersion, (GVD)], third-order dispersion (TOD), fourth-order dispersion (FOD), etc. Each term (and derivative) of the system is the sum of the terms introduced by the individual components (although nonlinear terms must be considered separately, as discussed below) i.e.,

$$\phi(\omega)=\sum_i \phi_i(\omega). \tag{10}$$

The group delay is defined by $T(\omega)\equiv\partial\phi(\omega)/\partial\omega$, and in physical terms is the transit time through the system for a group of quasimonochromatic waves.[54,82] Taylor expansion of the group delay gives

$$T(\omega)=\frac{\partial\varphi(\omega)}{\partial\omega}=\phi'(\omega_0)+\phi''(\omega_0)(\omega-\omega_0)+\tfrac{1}{2}\phi'''(\omega_0)(\omega-\omega_0)^2+\ldots\ldots. \tag{11}$$

From this expression, we see that when φ'' is nonzero, the pulse will have a linear frequency chirp, while a nonzero third-order dispersion (φ''') induces a quadratic chirp on the pulse, etc. The concepts of spectral phase and group delay are important for system design and modeling.

Typically, in an amplifier system consisting of a stretcher, amplifier(s), and compressor, we need to consider not only the contributions of the stretcher and the compressor, but also the materials of the amplifier, and possibly a prism pair or other elements which can be introduced to minimize higher-order dispersion. For example, the phase introduced by material is given by $\varphi_{\text{mat}}(\omega)=L_{\text{mat}}n(\omega)\omega/c$; empirical formulas for $n(\lambda)$ (such as Sellmeier equations) for common optical materials are tabulated (see, for example, Ref. 83). Since analytic derivatives are much more accurate than performing a numerical polynomial fit to a curve, it is most accurate to work with the exact expressions for the phase, and not with terms in the Taylor expansion. When a short pulse in the visible or near-infrared region passes through material, the longer wavelengths travel faster than the shorter wavelengths, thus introducing a positive chirp on the pulse. This chirp must also be compensated for by the pulse compressor. Table I gives expressions for the linear, quadratic, and cubic phase introduced by grating stretchers, compressors, prism pairs, and materials found in a typical amplifier, while Table II gives sample values for material (1 cm), grating pairs, and prism pairs.

TABLE I. Expressions for the linear, quadratic, and cubic phase introduced by grating stretchers; compressors, prism pairs, and materials found in a typical amplifier.

Order	Material	Grating pair compressor/stretcher	Prism pair
GVD	$\frac{d^2\phi_m(\omega)}{d\omega^2}=\frac{\lambda^3 L_m}{2\pi c^2}\frac{d^2n(\lambda)}{d\lambda^2}$	$\frac{d^2\phi_c(\omega)}{d\omega^2}=\frac{\lambda^3 L_g}{\pi c^2 d^2}\left[1-\left(\frac{\lambda}{d}-\sin\gamma\right)^2\right]^{-3/2}$	$\frac{d^2\phi_p(\omega)}{d\omega^2}=\frac{\lambda^3}{2\pi c^2}\frac{d^2P}{d\lambda^2}$
TOD	$\frac{d^3\phi_m(\omega)}{d\omega^3}=-\frac{\lambda^4 L_m}{4\pi^2 c^3}\left(3\frac{d^2n(\lambda)}{d\lambda^2}+\frac{\lambda d^3n(\lambda)}{d\lambda^3}\right)$	$\frac{d^3\phi_c(\omega)}{d\omega^3}=-\frac{6\pi\lambda}{c}\frac{d^2\phi_c(\omega)}{d\omega^2}\left(\frac{1+\frac{\lambda}{d}\sin\gamma-\sin^2\gamma}{\left[1-\left(\frac{\lambda}{d}-\sin\gamma\right)^2\right]}\right)$	$\frac{d^3\phi_p(\omega)}{d\omega^3}=\frac{-\lambda^4}{4\pi^2 c^3}\left(3\frac{d^2P}{d\lambda^2}+\lambda\frac{d^3P}{d\lambda^3}\right)$
FOD	$\frac{d^4\phi_m(\omega)}{d\omega^4}=\frac{\lambda^5 L_m}{8\pi^3 c^4}\left(12\frac{d^2n(\lambda)}{d\lambda^2}+8\lambda\frac{d^3n(\lambda)}{d\lambda^3}+\lambda^2\frac{d^4n(\lambda)}{d\lambda^4}\right)$	$\frac{d^4\phi_c(\omega)}{d\omega^4}=\frac{6d^2}{c^2}\frac{d^2\phi_c(\omega)}{d\omega^2}\left(\frac{80\frac{\lambda^2}{d^2}+20-48\frac{\lambda^2}{d^2}\cos\gamma+16\cos 2\gamma-4\cos 4\gamma+\frac{32\lambda}{d}\sin\gamma+\frac{32\lambda}{d}\sin 3\gamma}{\left(-8\frac{\lambda}{d}+\frac{4d}{\lambda}+\frac{4d}{\lambda}\cos 2\gamma+32\sin\gamma\right)^2}\right)-\frac{d^3\phi_c(\omega)}{d\omega^3}\frac{6\pi\lambda}{c}\left(\frac{1+\lambda/d\sin\gamma-\sin^2\gamma}{(1-(\lambda/d-\sin\gamma)^2)}\right)$	$\frac{d^4\phi_p(\omega)}{d\omega^4}=\frac{\lambda^5}{8\pi^3 c^4}\left(12\frac{d^2P}{d\lambda^2}+8\lambda\frac{d^3P}{d\lambda^3}+\lambda^2\frac{d^4P}{d\lambda^4}\right)$
			$P(\lambda)=L_p\cos\beta(\lambda)$ $\beta(\lambda)=-\arcsin(n_p(\lambda)\sin\alpha(\lambda))+\arcsin[n_p(\lambda_r)\sin\alpha(\lambda_r)]$ $\alpha(\lambda)=\xi-\arcsin[\sin\theta_b(\lambda)]/n_p(\lambda)$ $\theta_b(\lambda)=\arctan[n_p(\lambda)]$

To obtain a physical feel for the magnitude of the stretch factor, consider a 100 fs Gaussian input pulse incident on a pulse stretcher consisting of a 1200 grooves/mm grating, aligned at near-Littrow angle (28.7°) for a wavelength of 800 nm, and with an effective grating separation of 40 cm. The output pulse duration from the stretcher will be 120 ps. With no materials present in the amplifier (not a realistic situation!), then the phase contributions of the stretcher and compressor are identically equal and opposite to all orders, and perfect recompression of the output pulse to its original pulsewidth can be obtained (provided the imaging optics in the stretcher are aberration free, and that the spectral bandwidth of the pulse is not truncated). In order to compensate for dispersion introduced by materials in the amplifier, however, the compressor and stretcher angles and separation must be offset with respect to the ideal positions. Consider, for example, a typical regenerative amplifier system with a net amount of 44 cm of sapphire, 22 cm of silica, and 44 cm of KDP. If the incident angles in the stretcher and compressor are the same but the compressor grating separation is increased by 4.8 cm to compensate for the material, then the residual third-order dispersion will be 9×10^4 fs^3. This phase correction may be improved by adjusting the incident angle of either the stretcher or the compressor to make the ratio ϕ'''/ϕ'' equal to that of the material in the system. In some cases, the grating separation may then be set to simultaneously cancel second- and third-order phase errors, leaving only residual FOD. This approach has been demonstrated to work well in many TW-level laser systems which amplify 100 fs–1 ps duration pulses. For ultrashort-pulse systems, which seek to amplify the shortest pulses ($\approx$20 fs), more sophisticated approaches are needed to compensate for the residual high-order phase in order to obtain the shortest re-

TABLE II. Sample values of dispersion for material (1 cm), grating pairs, and prism pairs at 800 nm wavelength.

Optical element	GVD $d^2\varphi/d\omega^2$ (fs^2)	TOD $d^3\varphi/d\omega^3$ (fs^3)	FOD $d^4\varphi/d\omega^4$ (fs^4)
Fused silica	361.626	274.979	−114.35
BK7	445.484	323.554	−98.718
SF18	1543.45	984.277	210.133
KD*P	290.22	443.342	−376.178
Calcite	780.96	541.697	−118.24
Sapphire	581.179	421.756	−155.594
Sapphire at the Brewster angle	455.383	331.579	−114.912
Air	0.0217	0.0092	2.3×10^{-11}
Compressor: 600 ⁄/mm, $L=1$ cm, 13.89°	−3567.68	5101.21	−10226
Prism pair: SF18	−45.567	−181.516	−331.184

compressed pulses.[14–16,84,85] These approaches will be discussed below.

The factors that are important in the choice of grating period include the stretch factor required, compensation of higher-order dispersion, compactness, and the availability of high quality gratings of sufficient size, flatness, and diffraction efficiency. The stretch factor should be the minimum required to avoid damage to any coating and to avoid phase distortion due to nonlinear index of refraction of the sapphire. The damage threshold of a typical optical coating or multilayer dielectric mirror is $\sim 5\ \mathrm{J/cm^2} \times \tau_p^{1/2}$, where the pulse duration τ_p is measured in nanoseconds. For maximum extraction efficiency, the input fluence should be at or above the saturation fluence, which for Ti:sapphire, for example, is $1\ \mathrm{J/cm^2}$. This leads to a stretched pulse duration for Ti:sapphire in the range 40–200 ps. Nonlinear contributions to the phase resulting from self-phase modulation in the amplifier medium[86] must also be minimized to avoid self-focusing and self-phase modulation. The nonlinear phase shift is properly considered in the time domain, as $\phi_{\mathrm{NL}}(t) = (2\pi/\lambda) n_2 \int I(t,z)\,dz$. However, since the pulse is chirped inside the amplifier, this nonlinear temporal phase maps into the spectral phase. The approximate value of the nonlinear phase contribution is given by

$$\varphi_{\mathrm{nonlinear}}(t) = \int \frac{2\pi}{\lambda} n_2 I(t,l)\,dl, \tag{12}$$

where n_2 is the nonlinear index ($\approx 2.5\times 10^{-16}\ \mathrm{cm^2\,W^{-1}}$ for sapphire), and $I(t,l)$ is the intensity within the amplifier material. The peak value of this expression is also known as the ''*B* integral'' of the amplifier system. The value of the *B* integral (the nonlinear phase shift at peak intensity) at which the nonlinear phase is important for pulse compression can be estimated as follows. The nonlinear group delay is approximately $d\phi/d\omega = B/\Delta\omega$, where $\Delta\omega$ is the half-width of the amplified spectrum. A *B* integral of 1 rad over a spectral half-width of 20 nm would add an additional delay variation of 17 fs. While this may to some extent be compensated by readjustment of the compressor, the value of the nonlinear phase varies across the beam, so severe distortions may still occur. Thus, it is clearly advantageous where possible to maintain the value of the *B* integral at less than 1. From Table I, we see that the stretch (or chirp) in time that is introduced onto the input pulse by the stretcher gratings scales quadratically with the grating period. Thus, by doubling the grating period, we can increase the duration (and thus decrease the peak intensity) of the stretched pulse by a factor of 4 to eliminate damage and nonlinear effects.

The grating period will also determine the duration of the final compressed pulse because higher grating periods will introduce higher values of uncompensated higher-order dispersion. As discussed above, adjustment of the grating angles and the separation allows for some range of adjustment of second- and third-order phases, but compensation is not achievable for arbitrary groove spacing while still maintaining high throughput through the compressor. While high-groove density gratings are highly efficient, they generally introduce large third-order errors. A grating/prism stretcher design[87] allows direct compensation of third-order phase for this situation, but large values of fourth-order errors may still remain. In general, low groove density gratings allow simultaneous compensation of GVD TOD, with relatively low residual FOD, which can be eliminated if ultrashort duration output pulses are desired.[14–16,85] A final consideration in selecting a grating is that the larger the stretch factor, the larger the required grating size because the beam is spectrally dispersed on one of the gratings. However, large size, optically flat gratings are extremely difficult to manufacture to the required tolerances ($\lambda/10$). Therefore, very large stretch factors are not ideal—it will be more difficult to recompress the pulse after amplification, there will be increased sensitivity to alignment,[88] and the beam quality may be compromised. Generally the optimum groove density for TW Ti:sapphire systems is between 600 and 1200 grooves per mm.

B. Amplification

Prior to the late 1980s, traditional approaches to the amplification of ultrashort pulses relied on the use of organic dye or excimer amplifiers.[89–92] These systems were limited to output pulses of tens of millijoules because of the low saturation fluences associated with these amplifier media

$$J_{\mathrm{sat}} = \frac{h\nu}{\sigma_g}, \tag{13}$$

where ν is the transition frequency, σ_g is the gain cross section, and h is Plank's constant. For broadband laser dyes or gases, typical saturation fluences are $\approx 1-2\ \mathrm{mJ\,cm^{-2}}$. Thus, in order to extract a mere 5 mJ of amplified energy in a relatively short pulse, amplifier diameters of 2 cm or more were required. Therefore, since the late 1980s (following the availability of ultrashort-pulse solid-state laser sources at the appropriate wavelengths), most high-power ultrafast lasers have used solid-state amplifier media, including titanium-doped sapphire, Nd:glass, alexandrite, Cr:LiSAF, and others.[93] These materials have the combined advantages of relatively long upper level lifetimes, high saturation fluences ($\approx 1\ \mathrm{J\,cm^{-2}}$), broad bandwidths, and high damage thresholds. To date, most high-power ultrafast lasers have used either frequency-doubled YAG and glass lasers or flashlamps as pump sources for these amplifiers.

Of all potential amplifier media, titanium-doped sapphire, a material developed by Moulton in the early 1980s,[94,95] has seen the most widespread use in the past five years. It has several very desirable characteristics which make it ideal as a high-power amplifier material, including a very high damage threshold ($\approx 8-10\ \mathrm{J\,cm^{-2}}$), a high saturation fluence ($\approx 0.9\ \mathrm{J\,cm^2}$), a high thermal conductivity (46 W/mK at 300 K), and a suitable peak gain cross section of $\sigma_g \approx 2.7\times 10^{-19}\ \mathrm{cm^2}$. Therefore, pulses with an energy >1 J can be extracted from a relatively small diameter rod ($1\ \mathrm{cm}\times 1\ \mathrm{cm}$), and the gain is sufficiently high that only 12–15 passes through only three amplifier stages are required to reach this energy level. Moreover, it has the broadest gain bandwidth of any known material (230 nm), shown in Fig. 4, and thus can support an extremely short pulse. Finally, it has a broad absorption maximum at 500 nm (σ_{abs} at peak $\approx 6.5\times 10^{-20}\ \mathrm{cm^2}$), making it ideal for frequency-

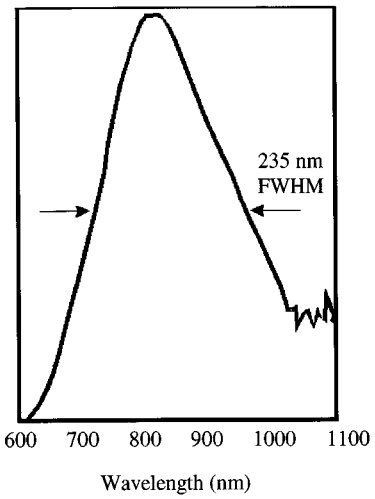

FIG. 4. Gain cross section of titanium-doped sapphire. (From Ref. 95.)

doubled YAG pump lasers. This is convenient since the radiative lifetime at $\approx 3\ \mu$s is too short for flashlamp pumping. Titanium concentrations of 0.05–0.25 wt % are typically used in laser and amplifier crystals. Since the sapphire host is birefringent, the Ti:sapphire crystal must be cut so that both the pump laser and amplified pulse polarization are along the crystal c axis, since the gain cross section is highest in this direction.

As well as increasing the pulse energy, the amplification process can significantly shape and shift the spectrum of the pulse. This is due to the finite gain bandwidth of the amplifier material, even though, as in the case of Ti:sapphire, this can be quite large. Since the gain cross section, $\sigma(\omega)$, appears in the exponent in calculating the amplification factor, successive passes through the amplifier tends to narrow the amplified spectrum, as can be seen from

$$n(t,\omega)=n_i(0,\omega)e^{\sigma(\omega)\Delta N}, \tag{14}$$

where ΔN is the total excited state population along the beampath, and $n(t,\omega)$ is the amplification factor. This spectral narrowing associated with the amplification process is referred to as gain narrowing. Figure 5(a) shows the amplified output pulse spectrum resulting from a gain of a factor of 10^7, assuming an infinitely broad and flat input spectrum, and no pump depletion. Even with a ''white light'' input, the output bandwidth is 47 nm. The finite gain cross section of the amplifier medium can also red- or blueshift the pulse, depending on the initial offset of the center wavelength of the input pulse relative to the peak of the gain. Figure 5(b) shows the input and output in the case of a spectrally shifted input pulse, with sufficient bandwidth to support an 11 fs pulse. In this example, the input spectrum was positioned optimally at 760 nm to ensure a maximum amplified pulse bandwidth. Since the gain profile of Ti:sapphire falls more steeply at wavelengths shorter than 800 nm than at wavelengths longer than 800 nm, and since gain saturation tends to redshift the spectrum (red wavelengths precede blue in the pulse), the optimum input spectrum is peaked shorter than 800 nm. This spectral shifting and reshaping is even more severe for narrower-bandwidth gain media. Figure 5(c) shows the additional narrowing which occurs in the case of a nonoptimally positioned input, where the bandwidth shrinks to 36 nm.

Finally, for large amplification factors, once the amplified pulse intensity becomes comparable to the saturation intensity of the medium, the pulse will experience amplification which is dependent on the transient excited-state population. This gain saturation, assumed to be dominated by homogeneous broadening, can be calculated from[96]

$$g=\frac{g_0}{1+E/E_{\mathrm{sat}}}, \tag{15}$$

where g is the gain, g_0 is small signal gain, E is the signal fluence, and E_{sat} is the saturation fluence (≈ 0.9 J/cm^2 for Ti:sapphire). In the case of a long-duration chirped pulse, the leading edge of the pulse depletes the excited-state population so that the red leading edge of the pulse can experience a higher gain than the blue trailing edge of the pulse. A set of nonlinear time-dependent equations is needed to fully model this gain-depletion and saturation process in the presence of gain narrowing, since gain narrowing acts in the frequency domain, whereas gain depletion acts in the time domain. It should be noted that gain narrowing, spectral shifting, and gain saturation occur in all amplifier media, and are least severe for broadband materials such as Ti:sapphire. For very short sub-30 fs pulses, gain narrowing (and the related prob-

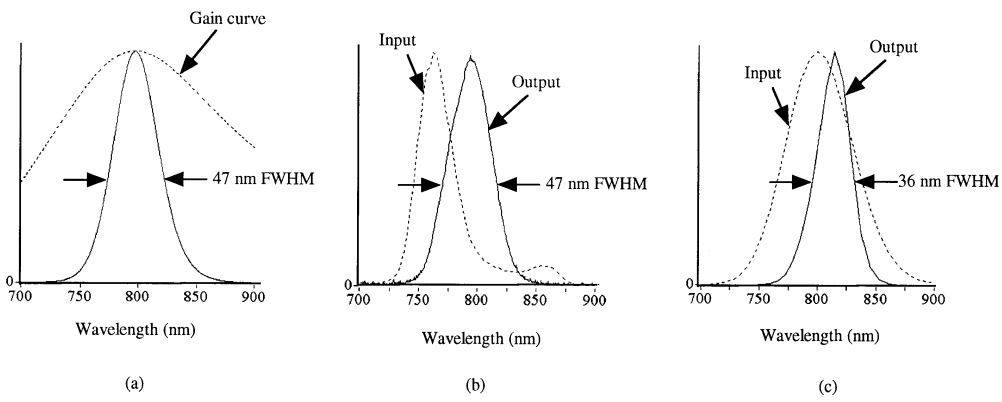

FIG. 5. Gain narrowing for the case of (a) an infinitely broad and flat input spectrum, (b) an optimally offset and shaped input spectrum, and (c) a nonoptimum input spectrum.

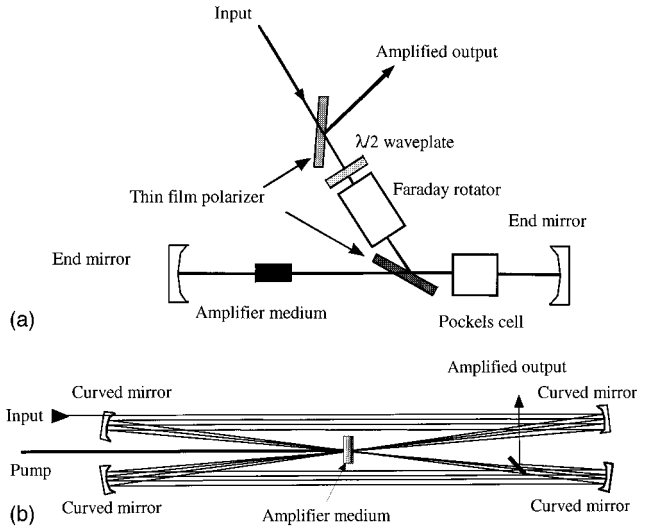

FIG. 6. Schematic diagram of (a) a regenerative preamplifier and (b) a multipass preamplifier.

lem of gain dispersion) can represent a severe limitation on the amplified bandwidth, restricting the amplified spectrum to values corresponding to a 20–30 fs pulse, depending on the exact amplification factor. (This is in contrast to the low energy, sub-10 fs output from Ti:sapphire lasers). However, the presence of gain narrowing is not a fundamental limitation on the amplified pulsewidth, as discussed below.

C. High-gain preamplifiers

Most high-power ultrafast laser systems use a high gain preamplifier stage, placed just after the pulse stretcher, which is designed to increase the energy of the nJ pulses from the laser oscillator to the 1–10 mJ level.[14,16,19,97–102] The majority of the gain of the amplifier system ($\approx 10^7$ net) occurs in this stage. The preamplifier is then followed by several power amplifiers designed to efficiently extract the stored energy in the amplifier and to increase the output pulse power to the multiterawatt level. There are two basic preamplifier designs, regenerative and multipass, and many variants thereof. These are illustrated in Figs. 6(a) and 6(b). Regenerative amplifiers (regens) are very similar to a laser cavity or resonator. The low-energy chirped pulse is injected into the cavity using a time-gated polarization device such as a Pockels cell and thin film polarizer. The pulse then makes ≈ 20 roundtrips through a relatively low gain medium, at which point the high energy pulse is switched out by a second time-gated polarization rotation. A low gain configuration is typically used in the regen cavity to prevent amplified spontaneous emission (ASE) buildup. With high gain, ASE can build up quite rapidly in a regen configuration and deplete the gain before it can be extracted by the short pulse. The beam overlap between the pump and signal pulse is usually quite good in a regen, which results in extraction efficiencies of up to 25%. Regenerative amplifiers are typically used as front ends for larger, long-pulse (50–100 fs) high-power laser systems. This is because the relatively long optical path lengths associated with the multiple passes in the regen cavity together with the presence of high-index materials due to the Pockels cells and polarizers can add high-order dispersion to an amplifier system, making it more difficult to recompress very short pulses. Nevertheless, regenerative amplifiers have also been used to generate pulses of 30 fs and shorter durations.[102–104]

A multipass preamplifier configuration differs from the regenerative amplifier in that, as its name suggests, the beam passes through the gain medium multiple times without the use of a cavity, as shown in Fig. 6(b). The particular geometry for accomplishing this can differ from system to system;[14–16,97,98] the configuration shown was first used in dye lasers by Hirlimann *et al.*,[105] and applied to high-power solid-state laser amplification by Backus and co-workers.[16] In a multipass amplifier, since the optical path is not a resonator, ASE can be suppressed to a greater degree than with a regenerative amplifier. Thus, multipass amplifiers typically have higher gain per pass (≈ 10) compared with regens, and fewer passes through the gain medium are needed. As a result, there is less high-order phase accumulation in multipass systems, and shorter pulses are easier to obtain upon recompression. Moreover, nonlinear phase accumulation due to the B integral is also less in multipass amplifiers. Multipass preamplifiers are not as efficient as regens, since the pump–signal overlap must change on successive passes through the gain medium in order to extract the beam (by separating it spatially). However, multipass preamplifier efficiencies can reach $\approx 15\%$, whereas multipass power amplifier efficiencies can reach $\approx 30\%$.[106]

IV. SPECIFIC LASER SYSTEMS

A. High repetition-rate systems

The availability of high average power pump lasers combined with the very high thermal conductivity of Ti:sapphire make it possible to construct millijoule-energy ultrafast laser systems which operate at kHz repetition rates.[16,19,99] In the past, such systems delivered 50–150 fs pulses at the mJ level.[19,99] More recently, high repetition rate systems have been demonstrated which deliver pulse energies of 3–5 mJ with pulse durations of ≈ 20 fs.[16,106] A system diagram for this laser is shown in Fig. 7. Since the output beam quality can be excellent, it is possible to generate peak powers of a fraction of a TW, with focusable intensities in excess of 10^{17} W cm^{-2} from such systems. These intensities are sufficient for most high-field atomic and plasma physics experiments. These high average power systems represent a significant advance in technology since, as recently as the late 1980s, such intensities were only barely accessible using low repetition-rate systems ($\leqslant 10$ Hz).[90]

Although Ti:sapphire has extremely high thermal conductivity, significant attention must still be devoted to reducing thermal distortion effects associated with the fact that tens of watts of average power are focused to $\sim$mm diameter in the laser amplifier to obtain sufficient gain per pass. These include thermal lensing, birefringence, and stress. The quantum efficiency for Ti:sapphire pumped by 527 nm light is ≈ 0.6, and therefore 40% of the absorbed light will be released as heat. A flat top pumping profile results in a parabolic thermal gradient and index of refraction variation

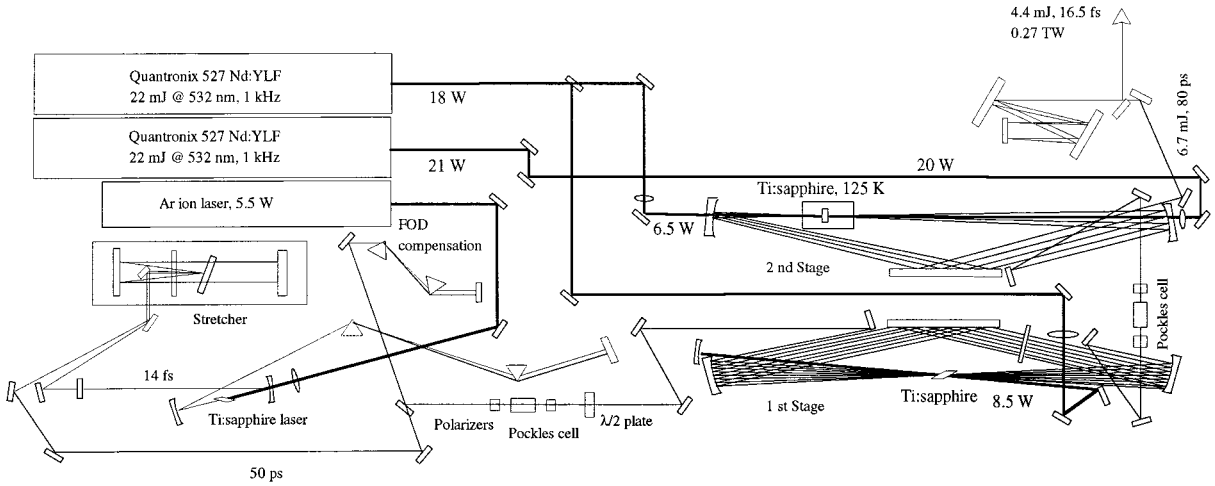

FIG. 7. Schematic diagram of a kHz repetition rate, 0.2 TW Ti:sapphire CPA system.

across the beam, which acts as a lens whose focal length varies with pump energy. Local thermal expansion stress and bowing of the crystal surface add to the lensing effect, as well as to thermally induced birefringence.

In multipass or regenerative amplifier systems, thermal lensing accumulates from successive passes through the amplifier, causing a rapid increase in amplified beam size. This in turn leads to a decrease in the focused spot size within the gain medium, causing the pulse to reach saturation fluence before all of the energy is extracted. In regens, the cavity can be designed to compensate for the thermal lens in a manner similar to that in laser oscillators. This can be done also in multipass amplifiers. Alternatively, an aperture mask can be employed[106] to restrict the transverse beam divergence or the crystal can be cooled to <-140 °C, since at low temperature the thermal conductivity is increased by an order of magnitude.[107,108]

B. High energy systems

For pulse energies larger than a few millijoules, amplification must be accomplished at lower repetition rate. Amplification in Ti:sapphire to pulse energies of 1–5 J is at present feasible; for larger pulse energies, refinement of crystal growth techniques for large aperture Ti:sapphire will be necessary. The first high-energy Ti:sapphire lasers used synchronously pumped dye laser sources, and generated pulses of ~100 fs and 50–500 mJ energy.[11,12] More recently, the development of ultrashort-pulse Ti:sapphire lasers has made it possible to generate pulses of up to 25 TW peak power with 20–30 fs durations.[14,15,17,85,104] The development of very high-energy Ti:sapphire lasers pumped by large Nd:glass lasers is also under development.[109]

For a number of applications, such as some short-wavelength laser schemes,[110] picosecond x-ray generation using laser-produced plasmas[111–113] and the ''fast ignitor'' concept in ICF physics,[51] high pulse energy is required at a more modest pulse duration (~0.5–1 ps). For these applications, Nd:glass is the laser medium of choice since it has a gain bandwidth sufficient for ≈400 fs pulse amplification and since the technology for large aperture amplifiers has already been developed for ICF studies. Despite the larger scale of these lasers, the basic CPA design of Fig. 1 is still applicable. Indeed, CPA was first implemented using Nd:glass amplification.[9] These early systems used Nd:YAG or Nd:YLF modelocked lasers, combined with fiber pulse compression, to generate ps duration seed pulses. However, since Ti:sapphire has an appreciable gain in the 1.05–1.06 μm region, the direct generation of 100 fs pulses in this wavelength region has proven to be preferable,[13] and nearly all current systems use a Ti:sapphire oscillator and preamplifier. For preamplification, the gain of Ti:sapphire is significantly lower at 1.06 μm than at 800 nm, necessitating a number of design modifications.[114] More passes through the gain medium are required, making only regenerative amplifiers practical. Care must be taken to suppress parasitic oscillation at 800 nm in the regenerative amplifier. However, the gain versus frequency profile for Ti:sapphire in the infrared is relatively flat compared with the gain profile near the 800 nm peak. This property, combined with the modest pulse duration requirement for Nd:glass, virtually eliminates gain narrowing in the preamplification process, making it possible to generate high-energy pulses with the duration limited solely by the gain bandwidth of Nd:glass. This bandwidth can be maximized by simultaneously using differing glass host materials in the amplifiers, thus broadening the aggregate gain profile.[115,116]

High-energy amplification of pulses emerging from the preamplifier is accomplished in an amplifier chain very similar to those used in ICF laser systems. Nd:glass rod amplifiers are used to amplify to energies of tens of joules, with Nd:glass disk amplifiers used for the largest diameter amplifier stages. Vacuum spatial filters are used between stages to maintain beam quality. Since the total material path length through the regenerative amplifier and the glass rod and disk amplifiers can be orders of magnitude larger than in the case of TW-level Ti:sapphire amplifiers, and since the saturation fluence is significantly higher,[93,107] nonlinear distortion (the B integral) is much more significant in these systems. This necessitates stretching the pulse to significantly longer durations than in the case of Ti:sapphire, with pulse stretching to

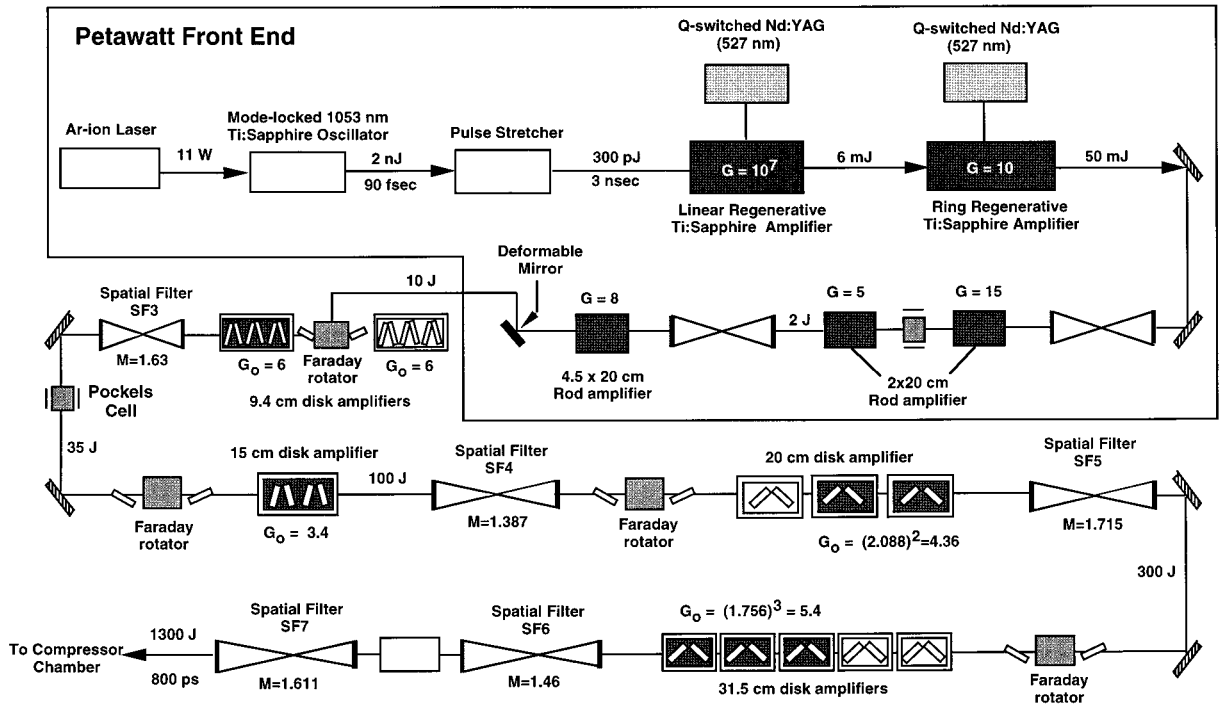

FIG. 8. Schematic diagram of a high-energy petawatt laser system in operation at Lawrence Livermore National Laboratory. This laser generates >600 J pulse energy in <500 fs using one beamline from the NOVA fusion laser facility. (Diagram courtesy of B. C. Stuart and M. D. Perry, LLNL.)

3 ns being practical at present.[18] Since the fractional bandwidth of these pulses is smaller than for ultrashort-pulse systems, stretching to long duration requires the use of very high groove-density gratings, high angles of incidence, and a large (several meters) inter-grating separation. In recompression, the high energy of these pulses requires large aperture optics. A primary limiting factor in these systems has thus been the availability of high optical quality, high damage threshold, large aperture diffraction gratings. This problem has been addressed through the development of new holographic gratings designed specifically for this application. High groove-density gratings with very high diffraction efficiency (up to 96% per reflection) can be fabricated using either a dielectric or a metal reflective layer. Although it had been hoped that dielectric coatings would be able to sustain much higher fluence without damage than the more common gold-coated grating, it was found that the primary damage mechanism is ionization and ablation of the surface, and not thermal heating due to linear absorption of the light.[117] The result is that the damage threshold of dielectric gratings is only modestly better than for gold. However, design of gold-coated gratings specifically for CPA, along with stringent fabrication techniques and process control, have made it possible to produce excellent, broadband, gold-coated gratings with working fluences of >300 mJ/cm^2.[18,118]

The application of this technology has resulted in a number of unique experimental facilities. Researchers at Lawrence Livermore National Laboratory (LLNL) have reported[18] the generation of pulses with peak power of up to 1.25 petawatts (600 J energy in <500 fs)[119] in a beam with good focusing properties, making it possible to generate peak intensities of over 10^{21} W/cm^2. CEA-Limeil has developed a 30–50 TW (24 J) in 440 fs system,[120] while Rutherford Appleton Laboratory has developed a 35 TW, 2 ps laser.[121] These systems all operate at low (a few pulses per hour) repetition rate. A schematic of the petawatt laser at LLNL is shown in Fig. 8.

Other amplification media have also been used for very high-energy systems, and new technologies promise to reduce or eliminate some of the present trade-offs. Chromium-doped LiSAF,[122] a material which is also of interest for compact, low-power ultrafast oscillator[123] and amplifier systems[124] because it can be pumped by laser diodes at 670 nm, has been used in medium aperture (25 mm) flashlamp-pumped amplifier systems to generate pulses of up to 1 J in as short as 70 fs.[125–129] This technology is limited primarily by the limited aperture size of the amplifier, by the poor thermal conductivity of LiSAF which limits repetition rate, and by materials quality and durability issues. However, the very broad gain bandwidth, from 780 to nearly 1000 nm, which overlaps Ti:sapphire, makes this material promising for ultrashort-pulse (50–100 fs) generation at the joule level when LiSAF growth and polishing techniques mature.

Another material with desirable characteristics for application to CPA is ytterbium-doped glass. Yb:glass operates at wavelengths around 1.05 μm, but has a broader bandwidth (>50 nm) and a higher saturation fluence ($\approx$30 J/cm^2) than Nd:glass.[130,131] Ultimately, pulse durations of $\sim$40 fs and energy extraction of up to damage threshold should be possible using this material, with very large aperture systems being in principle possible. The major challenges in implementation of this material are that (1) efficient energy extraction will require stretched pulse durations of 10 ns, and (2) the relatively narrow absorption bandwidth makes laser pumping,

rather than flashlamp pumping, necessary. Regarding (1), for efficient pulse compression, CPA requires diffraction gratings with dimensions comparable to or greater than $ct_{\text{stretched}}$, or 0.3 m/ns. Thus, new CPA technologies will be necessary to fully utilize this material. Regarding (2), although the absorption band is convenient for laser diode pumping, the cost of a diode-pumped high-energy amplifier system is currently prohibitive. Alternatively, Yb:glass can be pumped by a tunable Ti:sapphire or Cr:LiSAF laser. In any of these cases, the small quantum defect of Yb:glass dramatically reduces the heat load on the laser material, and thus operation at significantly higher repetition rates than lamp-pumped Nd:glass should be possible. Using laser pumping, the optical path length through the amplifiers can also be limited, mitigating nonlinear effects. Thus, even using current CPA techniques, amplification in Yb:glass may have desirable characteristics.

Ti:sapphire and Nd:glass lasers both operate in the near infrared. For many experimental applications of such high-power pulses, resonant, frequency-dependent effects play a minor role, and thus tunability is of secondary concern. However, many other applications in nonlinear optics, or the use of the laser output for ultrafast chemistry or solid-state studies, do require tunability. Furthermore, high-intensity sources at short wavelengths are desirable simply because the focal spot size can be significantly smaller, making it possible to generate much higher peak intensities for a given power. Frequency doubling of the output from Nd:glass and Ti:sapphire lasers can in some cases be quite efficient,[132–134] and can enhance the peak-to-background contrast of the pulses as well, which is usually desirable. Optical parametric amplifiers can create widely tunable ultrafast sources in the visible and infrared, and third- and fourth-harmonic generation can generate light in the ultraviolet (UV) with considerably reduced pulse energy.[135] In the UV, high material dispersion makes phase-matched harmonic generation in birefringent materials difficult for sub-100 fs pulses. Phase-matching issues can be minimized using third-harmonic generation in dilute gases, which makes it possible to generate pulses as short as 16 fs in the UV at microjoule energies.[26] However, the generation of terawatt peak-power pulses in the UV requires direct amplification schemes and new materials. Solid-state cerium-doped amplifier materials operate in the UV (at 290 nm), and can support 10 fs pulse duration.[136] However, lasers using these materials are at an early stage of development. The use of excimer laser gain media is a considerable more mature technology. The KrF excimer laser at 248 nm can deliver pulses $\leqslant$100 fs, and although the saturation fluence of this medium is low ($\approx$ mJ/cm^2), large aperture amplifiers are possible. Early excimer-laser based laser systems did not use CPA,[91,92,137,138] they used modelocked dye lasers, coupled with pulse amplification in dyes and frequency doubling or tripling to generate seed pulses for amplification in excimers. However, more recently, the preamplification stages have been more reliably implemented using Ti:sapphire oscillators and CPA amplifiers operating at 744 nm, followed by frequency tripling and injection into the amplifier.[139–141] A modest amount of chirping and subsequent recompression of the ultraviolet pulse has been found to be useful to obtain optimal energy extraction while avoiding two-photon damage effects in the optics of the amplifier chain.

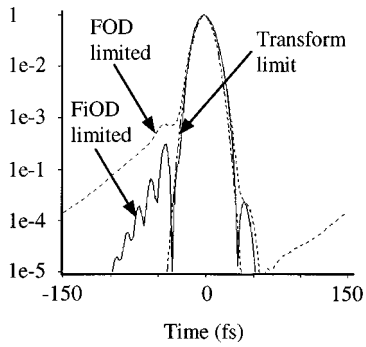

FIG. 9. Distortion of a 20 fs pulse with fourth- and fifth-order residual dispersions.

C. Ultrashort-pulse systems

In the development of amplifier systems for high-power pulses with duration $\leqslant$100 fs, there are two major effects which may limit the final pulse duration. First, as discussed above, the finite bandwidth of the gain medium results in narrowing of the pulse spectrum during amplification. Ti:sapphire is the broadest bandwidth laser material known (FWHM gain bandwidth of 230 nm); however, upon amplification by factors of $>10^7-10^{11}$, gain narrowing limits the output. As was shown in Fig. 5(a), assuming infinitely broadband input pulses injected into a Ti:sapphire amplifier with a gain of 10^7, the amplified output spectrum is $\approx$47 nm FWHM. This bandwidth is capable of supporting pulses as short as 18 fs at millijoule pulse energies. For tens of millijoules energy, the gain-narrowing limit is $\approx$25 fs. For all other materials, the gain-narrowing limit is more severe. Although techniques for ameliorating the effects of gain narrowing exist, these techniques at present provide only modest reduction in pulse duration, at the expense of significantly increased complexity.[35,85,116]

The second limiting effect on pulse duration is higher-order dispersion. The CPA technique requires very accurate chirping and compressing of a laser pulse, since the pulse stretching factors are in the range of 10^3-10^4. Higher-order dispersion is known to limit the pulse durations obtained from ultrashort-laser oscillators,[3,5,69,70] and the same considerations used in designing ultrashort-pulse oscillators also apply to amplifiers. For pulse durations $>$30 fs, both second- and third-order dispersion must be compensated. As discussed above, this compensation may be achieved by proper adjustment of the grating separation and incident angle. For shorter pulses, careful attention must be paid to sources of phase errors, and further modification to the system design must be made to minimize or cancel the fourth- and sometimes the fifth-order dispersions. Care must also be taken in alignment since higher-order dispersion can be introduced by, for example, a varying angle of incidence of the beam on the curved mirror in the stretcher. Figure 9 illustrates the distortion of a 20 fs pulse in the presence of fourth- and fifth-order residual dispersions, where the high-order uncom-

pensated dispersion introduced unwanted pedestals on the pulse. However, another degree of freedom is required to minimize FOD. The grating separation and angles can be adjusted to compensate second- and third-order dispersion, but in general there will still remain a positive residual fourth-order dispersion. Given that the contribution of most optical materials to the fourth-order is negative, material can be added to the beam path to cancel FOD.[81]

The choice of grating period significantly influences the magnitude of the residual FOD. For a constant GVD, the magnitudes of the TOD and FOD increase as the grating groove density is increased. The groove densities most commonly used in ultrashort-pulse CPA systems are 600 and 1200 ℓ/mm. Zhou *et al.* found that for the typical amount of material present in the beam path of a multipass amplifier system, the residual FOD was minimized by using 600 ℓ/mm gratings.[14,15] Yet another possibility is to use different groove densities for the stretcher and compressor,[142] although this choice is somewhat system specific. White *et al.*[84] designed a lens-based stretcher in which the second-, third-, and fourth-order dispersion may be controlled independently, at least for the tested bandwidth of 40 nm. Recently we found that by using an additional prism pair in the amplifier we could eliminate all higher-order dispersion over extremely large bandwidths to produce high-quality, 20 fs pulse durations.[106] Other possibilities for dispersion compensation exist, such as the design of special multilayer dielectric mirrors,[143] or even active control over the spectral phase in a spatially dispersed portion of the system.[144,145]

The choice of stretcher design is also important for ultrashort-pulse amplifier systems. There are two ''abberation-free'' reflective stretcher designs, the Offner triplet,[79,146] and a spherical mirror, all-reflective system.[106] Other designs[81,84] require that a ray trace of the system be performed to determine the predicted departure from ideal group delay, which is then compensated for. Whatever design is chosen, the stretcher must be carefully aligned to ensure there is no spatial chirp on the output beam. Wherever possible, all-reflective optics should be used in the system. However, even multilayer dielectrics add to the group delay variation in the amplifier system, and must be characterized for ultrashort-pulse operation.[147] Finally, for all ultrashort-pulse CPA systems, modeling of the system is important to ensure not only that the required degree of compensation can be obtained but that the sensitivity to alignment and adjustments is realistic.

It is crucial to note that the most important limit to the final pulse duration is not just the spectral width, but the shape of the spectrum. Modulation in the spectrum will lead to modulation of the pulse, as will spectral clipping. These effects can be subtle but important, particularly for applications where high contrast (low pulse background) is desired. Even for a well-behaved spectrum, free of modulation or clipping, the full width at half-maximum spectrum bandwidth is only a very approximate guide to pulse duration. For example, the transform-limited pulse duration (assuming flat spectral phase) of a pulse with a spectral FWHM of 40 nm will be approximately 18, 24, or 45 fs FWHM for sech^2, Gaussian, or flat-topped spectral shapes, respectively. Traditional autocorrelation techniques tend to underestimate the pulse duration since the spectrum is almost always always modulated or clipped, and thus the shape is never purely Gaussian or sech^2. Moreover, autocorrelation techniques require knowledge of the pulse shape in order to calculate the pulse duration, which is not known in advance, particularly when considering complex CPA systems. Furthermore, many experimental applications in nonlinear optics, such as high-harmonic generation[27] depend on the shape of the pulse electromagnetic wave form, on a cycle-by-cycle basis. Typically, the pulse width is extracted by assuming a ''pulse shape'' based upon the fit of the fast Fourier transform (FFT) of the measured spectrum. From this information, an autocorrelation factor is assumed to calculate the actual pulse duration. However, if the FFT of the measured spectrum is done improperly, the error in this type of estimation can be large. As an example, a Gaussian spectrum with a width of 50 nm corresponds to a transform-limited 20 fs pulse. In the presence of 1% additive white noise however, the pulse duration can be inaccurately calculated to be 10 fs due to the dc offset that the white noise introduces on the spectrum, giving rise to a delta function component to the pulse. These effects are illustrated in Fig. 10. To remove this type of error, a low

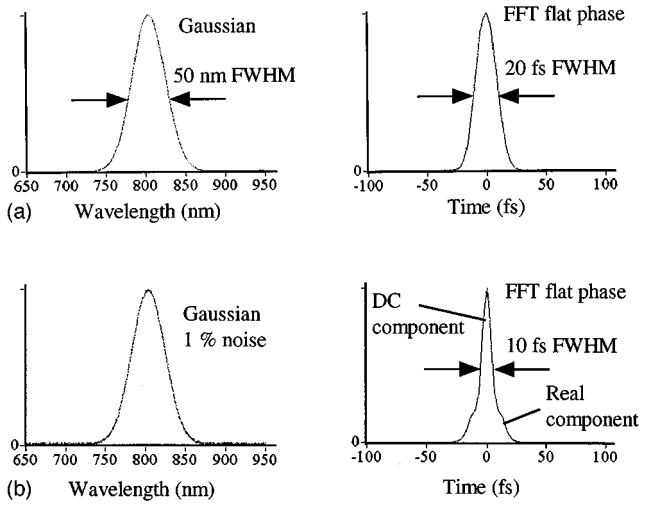

FIG. 10. Pulse spectrum and corresponding Fourier transform in the case of (a) a smooth Gaussian spectrum and (b) a Gaussian spectrum with 1% additive noise.

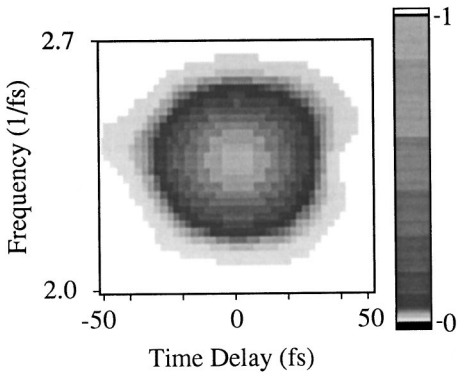

FIG. 11. Example of a FROG trace giving the spectrum and amplitude of the nonlinear signal as a function of delay.

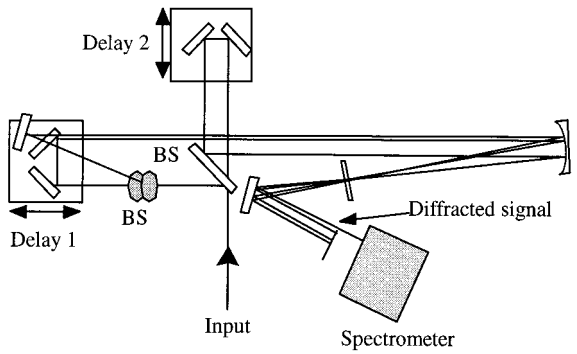

FIG. 12. Setup for transient grating frequency-resolved optical gating (TG-FROG).

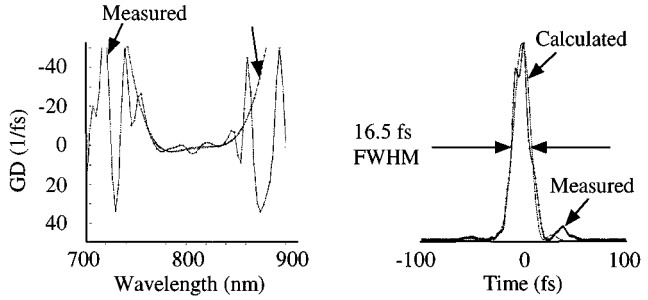

FIG. 14. A measured FROG trace of a 17 fs pulse from a CPA system including a loss-modulating pellicle to flatten the spectral variation of gain in the laser amplifier.

pass filter can remove the noise, together with a background subtraction to remove any dc offset.

In this light, the recent development of new measurement techniques, which allow complete characterization of ultrashort pulses, are a particularly significant development in the field. The technique of frequency-resolved optical gating (FROG)[148,149] retrieves both the amplitude and phase of a pulse, and has internal self-consistency checks on the data, which can greatly diminish the probability of measurement errors. Such techniques are the only reliable methods to use for the measurement of sub-30 fs pulses. In traditional autocorrelation techniques, the amplitude of a nonlinear signal is recorded as a function of the delay between two identical replicas of a short pulse. In FROG both the spectrum and amplitude of the nonlinear signal are recorded as a function of delay, and an example set of the data is shown in Fig. 11. This data can then be processed using fast computer algorithms to retrieve the spectrum and spectral phase of the pulse, from which the pulse amplitude and temporal phase can be calculated. The data shown in Fig. 11 were taken using the new technique of transient grating FROG, which generates a nonlinear signal when two beams are overlapped in fused silica (for example), and a third beam scatters off the induced grating from the first two beams to generate a nonlinear signal at the same frequency. The setup, shown in Fig. 12, is similar to a traditional autocorrelator, except that three beams must be generated so it is somewhat more complex.

Figure 13 shows the power of these FROG techniques when comparing the measured and calculated group delay, spectrum, and pulse shape, from an ultrashort-pulse CPA system. The measured curves were obtained by deconvolution of the data of Fig. 11. There is excellent agreement between measured (using FROG) and calculated (using computer models of the amplifier) data.[106] Such techniques are very important for future applications of ultrashort, high-power pulses since many high-intensity effects are very sensitive to the actual pulse shape. Figure 14 shows an example of another FROG trace obtained from this same laser amplifier system, but with a thin etalon inserted into the first-stage amplifier ring to reshape the spectral gain function in the amplifier. The use of this etalon narrows the pulse full width at half-maximum to 17 fs, while also adding small pre- and postpulses due to reshaping of the spectrum and the introduction of phase distortions by the etalon.

To reduce unwanted spectral clipping in ultrashort-pulse CPA systems, the optical elements must be chosen or designed to transmit as wide a bandwidth as possible. Calcite polarizers should be used instead of thin film polarizers wherever the power level permits. Zero-order or achromatic wave plates have substantially less retardation error over a broad bandwidth than do multiple-order wave plates. The gratings and mirrors (especially multilayer dielectrics) can also strongly shape the spectrum. All birefringent elements must be properly aligned to avoid secondary pulses as well as the corresponding modulation of the spectrum. (This is

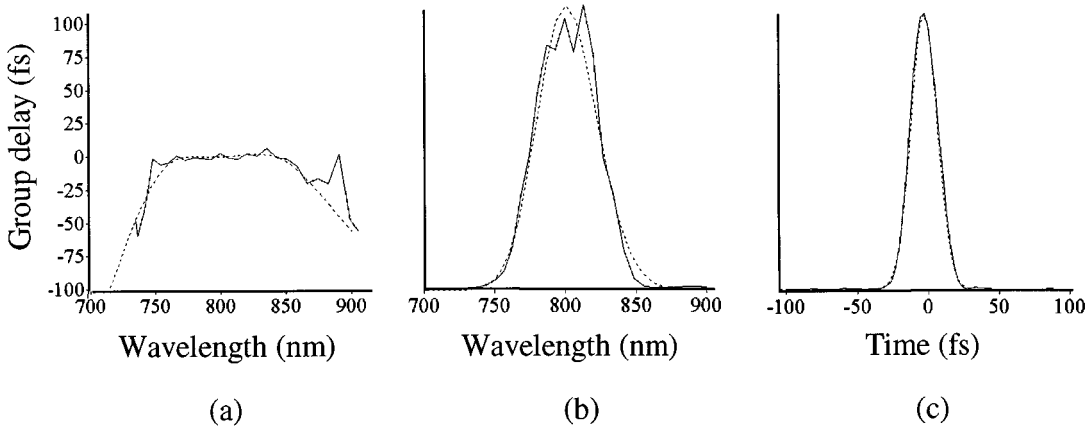

FIG. 13. Measured (using FROG) and calculated (using computer models) output from a ultrashort-pulse 20 fs CPA system: (a) group delay, (b) pulse spectrum, (c) pulse duration. The measured curves were obtained through a deconvolution of the FROG data of Fig. 11.

especially noticeable when a half-wave plate/polarizer combination is used to attenuate the pulse energy. An additional polarizer may also be used to clean up the polarization before the attenuator to avoid this problem.) Finally, the stretcher (and prism pair, if needed) must be carefully aligned. If the grating pair in a pulse compressor or stretcher is not parallel, different colors of the output will be traveling in slightly different directions. This will cause a spatial chirp which is particularly noticeable when the pulse is tightly focused, which is usually what one is trying to do with the pulse.

As discussed above, gain narrowing during amplification limits the amplified pulse bandwidth. In the presence of gain saturation however, there is additional spectral shaping that results from the fact that the leading edge of the chirped pulse (longer wavelength) sees a higher gain than the trailing edge. To model this effect, the chirped pulse must be divided into short time slices, each with its own center frequency. The energy contained within each slice is small enough to use the small signal approximation (adjusted for the local frequency), while the energy extracted by each slice is subtracted from the stored energy in the crystal. The more amplification stages in a system, the more pronounced the redshift upon amplification. To reduce the effects of gain narrowing, the pulse injected to the amplifier must be shorter than the desired output pulse. The redshift due to gain saturation and some of the gain narrowing may be compensated by aligning the oscillator spectrum to the blue side of the desired output spectrum, as shown in Fig. 5(b). Gain narrowing may be further reduced by shaping the amplitude of the spectrum with a mask in the stretcher.[85] However, this has the disadvantage of introducing modulations into the spectrum, which result in poorly shaped output pulses with wings. An alternate method is to regeneratively shape the spectrum using intracavity elements such as a thin etalons.[103,104] Extremely broad bandwidths can be generated using this method, at the expense of the quality of the spectral shape and the phase characteristics of the pulse. Gain narrowing may also be actively defeated in special cases by using gain media with different frequencies of peak gain. This has successfully been shown in Nd:glass systems.[115] This scheme is difficult to implement for the ultrashort-pulse systems, but possible candidates include Cr:LiSAF and alexandrite. Yet another approach is a spatially dispersive amplification scheme[78] in which the beam is amplified while spatially dispersed, and the laser pump distribution is arranged to produce a flat spectral gain profile.

In addition to gain narrowing, there is another effect of gain dispersion because of the presence of inverted atoms in the gain medium changes the effective index of refraction. For a Lorentzian line profile, the amplifier phase shift is given by

$$\varphi(\omega)=\ln(G_{\mathrm{tot}})\ \frac{(\omega-\omega_0)/\Delta\omega_g}{1+4((\omega-\omega_0)/\Delta\omega_g)^2}. \tag{16}$$

For a gain of 10^6, gain dispersion results in a roughly parabolic variation in group delay, introducing a 10 fs delay between the line center and a point 50 nm away.

V. DISCUSSION

Progress in high peak-power ultrafast lasers has been rapid in the 1990s, and new developments promise to continue to create exciting progress for the forseeable future. The capabilities of laboratory-scale laser systems will continue to improve in terms of available average and peak power, and in terms of control and characterization of the electromagnetic field of the pulse on a cycle-by-cycle basis. Developments in other areas of laser technology, such as diode-pumped lasers and adaptive optics for spatial and temporal wave front control, can readily be incorporated into ultrafast systems. Scientifically, these developments may make possible optical ''coherent control'' of chemical reactions and quantum systems,[150–152] and will extend ultrafast optical science into the x-ray region of the spectrum. Ultrafast x-ray techniques will allow us to observe reactions on a microscopic temporal and spatial scale and to develop a fundamental understanding of the most basic processes underlying the natural world. On a more applied level, the cost and complexity of ultrafast lasers will decrease, making feasible the widespread application of ultrafast technology for industrial and medical applications such as precision machining, thin film deposition, optical ranging, and opthamological surgery. On a larger scale, we are currently at the threshold of generating petawatt peak power lasers. Clearly, the impetus for the development even larger scale lasers will be coupled with compelling scientific and societal needs, such as the prospect of laser-induced fusion energy or of laser-based particle accelerators or x-ray lasers. At present, we have reached neither the technological nor the fundamental limits of this technology.

ACKNOWLEDGMENTS

The authors would like to thank B. C. Stuart and M. D. Perry of Lawrence Livermore National Laboratory for supplying Fig. 8. The authors gratefully acknowledge support for their work from the National Science Foundation and the Department of Energy. One of the authors (H.C.K.) acknowledges generous support from an Alfred P. Sloan Foundation fellowship.

[1] D. E. Spence, P. N. Kean, and W. Sibbett, Opt. Lett. **16**, 42 (1991).
[2] M. M. Murnane and H. C. Kapteyn, IEEE LEOS Newsletter August 17 (1993).
[3] H. C. Kapteyn and M. M. Murnane, Opt. Photonics News **5**, 20 (1994).
[4] H. C. Kapteyn and M. M. Murnane, IEEE LEOS Newsletter August (1995).
[5] M. T. Asaki, C. P. Huang, D. Garvey, J. Zhou, H. C. Kapteyn, and M. M. Murnane, Opt. Lett. **18**, 977 (1993).
[6] J. Zhou, G. Taft, C. P. Huang, M. M. Murnane, H. C. Kapteyn, and I. Christov, Opt. Lett. **19**, 1149 (1994).
[7] A. Stingl, M. Lenzner, C. Spielmann, F. Krausz, and R. Sipocs, Opt. Lett. **20**, 602 (1995).
[8] I. P. Christov, V. Stoev, M. Murnane, and H. Kapteyn, Opt. Lett. **21**, 1493 (1996).
[9] D. Strickland and G. Mourou, Opt. Commun. **56**, 219 (1985).
[10] P. Maine, D. Strickland, P. Bado, M. Pessot, and G. Mourou, IEEE J. Quantum Electron. **24**, 398 (1988).
[11] A. Sullivan, H. Hamster, H. C. Kapteyn, S. Gordon, W. White, H. Nathel, R. J. Blair, and R. W. Falcone, Opt. Lett. **16**, 1406 (1991).
[12] J. D. Kmetic, J. J. Macklin, and J. F. Young, Opt. Lett. **16**, 1001 (1991).

[13] C. Rouyer, E. Mazataud, I. Allais, A. Pierre, S. Seznec, C. Sauteret, G. Mourou, and A. Migus, Opt. Lett. **18**, 214 (1993).
[14] J. P. Zhou, C. P. Huang, C. Shi, H. C. Kapteyn, and M. M. Murnane, Opt. Lett. **19**, 126 (1994).
[15] J. P. Zhou, C. P. Huang, M. M. Murnane, and H. C. Kapteyn, Opt. Lett. **20**, 64 (1995).
[16] S. Backus, J. Peatross, C. P. Huang, M. M. Murnane, and H. C. Kapteyn, Opt. Lett. **20**, 2000 (1995).
[17] J. P. Chambaret, C. LeBlanc, G. Cheriaux, P. Curley, G. Darpentigny, P. Rousseau, G. Hamoniaux, A. Antonetti, and F. Salin, Opt. Lett. **21**, 1921 (1996).
[18] B. C. Stuart, M. D. Perry, J. Miller, G. Tietbohl, S. Herman, J. A. Britten, C. Brown, D. Pennington, V. Yanovsky, and K. Wharton, Opt. Lett. **22**, 242 (1997).
[19] J. V. Rudd, G. Korn, S. Kane, J. Squier, and G. Mourou, Opt. Lett. **18**, 2044 (1993).
[20] A. McPherson, G. Gibson, H. Jara, U. Johann, T. S. Luk, I. A. McIntyre, K. Boyer, and C. K. Rhodes, J. Opt. Soc. Am. B **4**, 595 (1987).
[21] M. M. Murnane, H. C. Kapteyn, M. D. Rosen, and R. W. Falcone, Science **251**, 531 (1991).
[22] A. L'Huillier and P. Balcou, Phys. Rev. Lett. **70**, 774 (1993).
[23] J. J. Macklin, J. D. Kmetec, and C. L. Gordon III, Phys. Rev. Lett. **70**, 766 (1993).
[24] J. Zhou, J. Peatross, M. M. Murnane, H. C. Kapteyn, and I. P. Christov, Phys. Rev. Lett. **76**, 752 (1996).
[25] R. W. Schoenlein *et al.*, Science **274**, 236 (1996).
[26] S. Backus, J. Peatross, M. Murnane, and H. Kapteyn, Opt. Lett. **21**, 665 (1996).
[27] I. P. Christov, J. P. Zhou, J. Peatross, A. Rundquist, M. M. Murnane, and H. C. Kapteyn, Phys. Rev. Lett. **77**, 1743 (1996).
[28] J. R. Marques *et al.*, Phys. Rev. Lett. **76**, 3566 (1996).
[29] D. Umstadter, S.-Y. Chen, A. Maksimchuk, G. Mourou, and R. Wagner, Science **273**, 472 (1996).
[30] D. Umstadter, J. Kim, and E. Dodd, Phys. Rev. Lett. **76**, 2073 (1996).
[31] I. P. Christov, M. M. Murnane, and H. C. Kapteyn, Phys. Rev. Lett. **78**, 1251 (1997).
[32] Z. Chang, A. Rundquist, H. Wang, M. M. Murnane, and H. C. Kapteyn, Phys. Rev. Lett. **79**, 2967 (1997).
[33] C. Spielmann, N. H. Burnett, S. Sartania, R. Koppitsch, M. Schnürer, C. Kan, M. Lenzner, P. Wobrauschek, and F. Krausz, Science **278**, 661 (1997).
[34] R. Haight and D. R. Peale, Rev. Sci. Instrum. **65**, 1853 (1994).
[35] M. Nisoli, S. D. Silvestri, and O. Svelto, Appl. Phys. Lett. **68**, 2793 (1996).
[36] M. Nisoli, S. de Silvestri, O. Svelto, R. Szipocs, K. Ferencz, C. Spielmann, S. Sartania, and F. Krausz, Opt. Lett. **22**, 522 (1997).
[37] S. Backus, K. Read, C. Durfee, A. Braun, M. M. Murnane, and H. C. Kapteyn, Opt. Lett. (submitted).
[38] C. G. Durfee, S. Backus, M. M. Murnane, and H. C. Kapteyn, Opt. Lett. **22**, 1565 (1997).
[39] P. B. Corkum, N. H. Burnett, and M. Y. Ivanov, Opt. Lett. **19**, 1870 (1994).
[40] K. J. Schafer and K. C. Kulander, Phys. Rev. Lett. **78**, 638 (1997).
[41] H. C. Kapteyn and M. M. Murnane, ''Relativistic Pulse Compression,'' J. Opt. Soc. Am. B **8**, 1657 (1991).
[42] T. Tajima and J. M. Dawson, Phys. Rev. Lett. **43**, 267 (1979).
[43] A. Borisov, A. Borovskiy, V. Korobkin, A. Prokhorov, C. Rhodes, and O. Shiryaev, Phys. Rev. Lett. **65**, 1753 (1990).
[44] D. L. Matthews *et al.*, Phys. Rev. Lett. **54**, 110 (1985).
[45] S. Suckewer, C. H. Skinner, H. Milchberg, C. Keane, and D. Voorhees, Phys. Rev. Lett. **55**, 1753 (1985).
[46] B. J. MacGowan, S. Maxon, C. J. Keane, R. A. London, D. L. Matthews, and D. A. Whelan, J. Opt. Soc. Am. B **5**, 1858 (1988).
[47] M. A. Duguay and P. M. Rentzepis, Appl. Phys. Lett. **10**, 350 (1967).
[48] H. C. Kapteyn, Appl. Opt. **31**, 4931 (1992).
[49] E. J. Valeo and S. C. Cowley, Phys. Rev. E **47**, 1321 (1993).
[50] W. Leemans, R. Schoenlein, P. Volfbeyn, A. Chin, T. Glover, P. Balling, M. Zolotorev, K. Kim, S. Chattopadhyay, and C. Shank, Phys. Rev. Lett. **77**, 4182 (1996).
[51] M. Tabak, J. Hammer, M. Glinsky, W. Kruer, S. Wilks, J. Woodworth, E. Campbell, M. Perry, and R. Mason, Phys. Plasmas **1**, 1626 (1994).
[52] M. Pessot, P. Maine, and G. Mourou, Opt. Commun. **62**, 419 (1987).
[53] M. Pessot, J. Squier, P. Bado, G. Mourou, and D. J. Harter, IEEE J. Quantum Electron. **25**, 61 (1988).
[54] E. B. Treacy, IEEE J. Quantum Electron. **QE-5**, 454 (1969).
[55] O. E. Martinez, J. P. Gordon, and R. L. For, J. Opt. Soc. Am. A **1**, 1003 (1984).
[56] O. E. Martinez, J. Opt. Soc. Am. B **3**, 929 (1986).
[57] O. E. Martinez, IEEE J. Quantum Electron. **QE-23**, 1385 (1987).
[58] O. E. Martinez, IEEE J. Quantum Electron. **23**, 59 (1987).
[59] M. Ferray, L. A. Lompré, O. Gobert, A. L'Huillier, G. Mainfray, C. Manus, A. Sanchez, and A. S. Gomes, Opt. Commun. **75**, 278 (1990).
[60] W. H. Knox, J. Opt. Soc. Am. B **4**, 1771 (1987).
[61] B. Nikolaus and D. Grishkowsky, Appl. Phys. Lett. **252**, 2 (1983).
[62] J. A. Valdmanis and R. L. Fork, IEEE J. Quantum Electron. **QE-22**, 112 (1986).
[63] W. Joosen, H. J. Bakker, L. D. Noordam, H. G. Muller, and H. B. van Linden van den Heuvell, J. Opt. Soc. Am. B **8**, 2087 (1991).
[64] H. A. Haus, IEEE J. Quantum Electron. **QE-11**, 736 (1975).
[65] A. Stingl, M. Lenzner, C. Spielmann, F. Krausz, and R. Sipocs, Opt. Lett. **19**, 204 (1994).
[66] S.-P. Lasers and C. Lasers.
[67] R. L. Fork, O. E. Martinez, and J. P. Gordon, Opt. Lett. **9**, 150 (1984).
[68] I. P. Christov, H. C. Kapteyn, M. M. Murnane, C. P. Huang, and J. P. Zhou, Opt. Lett. **20**, 309 (1995).
[69] C. P. Huang, H. C. Kapteyn, J. W. McIntosh, and M. M. Murnane, Opt. Lett. **17**, 139 (1992).
[70] C. P. Huang, M. T. Asaki, S. Backus, M. M. Murnane, H. C. Kapteyn, and H. Nathel, Opt. Lett. **17**, 1289 (1992).
[71] L. Xu, C. Spielmann, F. Krausz, and R. Szipöcs, Opt. Lett. **21**, 1259 (1996).
[72] I. D. Jung, F. X. Kärtner, N. Matuschek, D. H. Sutter, F. Morier-Genoud, G. Zhang, U. Keller, V. Scheuer, M. Tilsch, and T. Tschudi, Opt. Lett. **22**, 1009 (1997).
[73] S. Cundiff, W. Knox, E. Ippen, and H. Haus, Opt. Lett. **21**, 662 (1996).
[74] I. P. Christov, Prog. Opt. **29**, 201 (1991).
[75] I. P. Christov, Opt. Commun. **53**, 364 (1985).
[76] I. P. Christov, M. M. Murnane, H. C. Kapteyn, J. P. Zhou, and C. P. Huang, Opt. Lett. **19**, 1465 (1994).
[77] I. P. Christov, V. Stoev, M. Murnane, and H. Kapteyn, Opt. Lett. **20**, 2111 (1995).
[78] I. P. Christov, Opt. Lett. **17**, 742 (1992).
[79] G. Cheriaux, P. Rousseau, F. Salin, J. Chambaret, B. Walker, and L. Dimauro, Opt. Lett. **21**, 414 (1996).
[80] A. Offner, U.S., 1971.
[81] B. E. Lemoff and C. P. Barty, Opt. Lett. **18**, 1651 (1993).
[82] S. D. Brorson and H. A. Haus, J. Opt. Soc. Am. B **5**, 247 (1988).
[83] M. Bass, *Handbook of Optics*, Optical Society of America (McGraw–Hill, New York, 1995).
[84] W. E. White, F. G. Patterson, R. L. Combs, D. F. Price, and R. L. Shepherd, Opt. Lett. **18**, 1343 (1993).
[85] C. P. J. Barty, C. L. Gordon III, and B. E. Lemoff, Opt. Lett. **19**, 1442 (1994).
[86] M. D. Perry, T. Ditmire, and B. Stuart, Opt. Lett. **19**, 2149 (1994).
[87] S. Kane, J. Squier, J. Rudd, and G. Mourou, Opt. Lett. **19**, 1876 (1994).
[88] C. Fiorini, C. Sauteret, C. Rouyer, N. Blanchot, S. Seznec, and A. Migus, IEEE J. Quantum Electron. **30**, 1662 (1996).
[89] R. L. Fork, C. V. Shank, and R. T. Yen, Appl. Phys. Lett. **41**, 223 (1982).
[90] M. M. Murnane and R. W. Falcone, J. Opt. Soc. Am. B **5**, 1573 (1988).
[91] A. P. Schwarzenbach, T. S. Luk, I. A. McIntyre, U. Johann, A. McPherson, K. Boyer, and C. K. Rhodes, Opt. Lett. **11**, 499 (1986).
[92] S. Watanabe, A. Endoh, M. Watanabe, N. Sarukura, and K. Hata, J. Opt. Soc. Am. B **6**, 1870 (1989).
[93] P. Moulton, Proc. IEEE **80**, 348 (1992).
[94] P. F. Moulton, MIT Lincoln Laboratory Report No. 1982:3 (1982).
[95] P. F. Moulton, J. Opt. Soc. Am. B **3**, 125 (1986).
[96] A. Yariv, *Quantum Electronics*, 3rd ed. (Wiley, New York, 1989).
[97] C. LeBlanc, G. Grillon, J. P. Chambaret, A. Migus, and A. Antonetti, Opt. Lett. **18**, 140 (1993).
[98] M. Lenzner, C. Spielmann, E. Wintner, F. Krausz, and A. J. Schmidt, Opt. Lett. **20**, 1397 (1995).
[99] F. Salin, J. Squier, G. Mourou, and G. Vaillancourt, Opt. Lett. **16**, 1964 (1991).
[100] J. Squier, S. Coe, K. Clay, G. Mourou, and D. Harter, Opt. Commun. **92**, 73 (1992).
[101] G. Vaillancourt, T. Norris, J. Coe, P. Bado, and G. Mourou, Opt. Lett. **15**, 317 (1990).

[102] K. Wynne, G. D. Reid, and R. M. Hochstrasser, Opt. Lett. **19**, 895 (1994).
[103] C. Barty, G. Korn, F. Raksi, C. Rose-Petruck, J. Squier, A. Tian, K. Wilson, V. Yakovlev, and K. Yamakawa, Opt. Lett. **21**, 219 (1996).
[104] C. Barty, T. Guo, C. Le Blanc, F. Raksi, C. Rose-Petruck, J. Squier, K. Wilson, V. Yakovlev, and K. Yamakawa, Opt. Lett. **21**, 668 (1996).
[105] C. Hirlimann, O. Seddiki, J.-F. Morhange, R. Mounet, and A. Goddi, Opt. Commun. **59**, 52 (1986).
[106] S. Backus, C. Durfee, M. M. Murnane, and H. C. Kapteyn, Opt. Lett. (submitted).
[107] W. Koechner, *Solid-State Laser Engineering* (Springer, Heidelberg, 1996).
[108] A. DeFranzo and B. Pazol, Appl. Opt. **32**, 2224 (1993).
[109] A. Sullivan, J. Bonlie, D. Price, and W. White, Opt. Lett. **21**, 603 (1996).
[110] H. C. Kapteyn, L. B. D. Silva, and R. W. Falcone, Proc. IEEE **80**, 342 (1992).
[111] J. Workman, A. Maksimchuk, X. Liu, U. Ellenberger, J. Coe, C. Chien, and D. Umstadter, J. Opt. Soc. Am. B **13**, 125 (1996).
[112] C. Chien, J. Coe, G. Mourou, J. Kieffer, M. Chaker, Y. Beaudoin, O. Peyrusse, and D. Gilles, Opt. Lett. **18**, 1535 (1993).
[113] M. M. Murnane, H. C. Kapteyn, and R. W. Falcone, Phys. Rev. Lett. **62**, 155 (1989).
[114] B. Stuart, S. Herman, and M. Perry, IEEE J. Quantum Electron. **31**, 528 (1995).
[115] M. D. Perry, F. G. Patterson, and J. Weston, Opt. Lett. **15**, 381 (1990).
[116] F. Patterson, R. Gonzales, and M. Perry, Opt. Lett. **16**, 1107 (1991).
[117] B. Stuart, M. Feit, S. Herman, A. Rubenchik, B. Shore, and M. Perry, J. Opt. Soc. Am. B **13**, 459 (1996).
[118] R. Boyd, J. Britten, D. Decker, B. Shore, B. Stuart, M. Perry, and L. Lifeng, Appl. Opt. **34**, 1697 (1995).
[119] M. D. Perry, Sci. Technol. Rev. December 4 (1996).
[120] C. Rouyer, N. Blanchot, I. Allais, E. Mazataud, J. Miquel, M. Nail, A. Pierre, C. Sauteret, and A. Migus, J. Opt. Soc. Am. B **13**, 55 (1996).
[121] C. Danson *et al.*, Opt. Commun. **103**, 392 (1993).
[122] M. Stalder, B. Chai, and M. Bass, Appl. Phys. Lett. **58**, 216 (1991).
[123] S. Tsuda, W. Knox, and S. Cundiff, Appl. Phys. Lett. **69**, 1538 (1996).
[124] R. Mellish, N. Barry, S. Hyde, R. Jones, P. French, J. Taylor, C. van der Poel, and A. Valster, Opt. Lett. **20**, 2312 (1995).
[125] P. Beaud, M. Richardson, E. J. Miesak, and B. H. T. Chai, Opt. Lett. **18**, 1550 (1993).
[126] P. Beaud, M. Richardson, and E. J. Miesak, IEEE J. Quantum Electron. **31**, 317 (1995).
[127] T. Ditmire and M. D. Perry, Opt. Lett. **18**, 426 (1993).
[128] W. E. White, J. R. Hunter, L. V. Woerkom, T. Ditmire, and M. D. Perry, Opt. Lett. **17**, 1067 (1992).
[129] T. Ditmire, H. Nguyen, and M. D. Perry, Opt. Lett. **20**, 1142 (1995).
[130] X. Zou and H. Toratani, Phys. Rev. B **52**, 15 889 (1995).
[131] H. M. Pask, R. J. Carman, D. C. Hanna, A. C. Tropper, C. J. Mackechnie, P. R. Barber, and J. M. Dawes, IEEE J. Sel. Top. Quantum Electron. **1**, 1 (1995).
[132] Y. Wang and R. Dragila, Phys. Rev. A **41**, 5645 (1990).
[133] Y. Wang and B. Luther-Davies, Opt. Lett. **17**, 1459 (1992).
[134] C. Y. Chien, G. Korn, J. S. Coe, J. Squier, G. Mourou, and R. S. Craxton, Opt. Lett. **20**, 353 (1995).
[135] J. Ringling, O. Kittelmann, F. Noack, G. Korn, and J. Squier, Opt. Lett. **18**, 2035 (1993).
[136] N. Sarukura, M. Dubinskii, L. Zhenlin, V. Semashko, A. Naumov, S. Korableva, R. Abdulsabirov, K. Edamatsu, Y. Suzuki, T. Itoh, and Y. Segawa, IEEE J. Sel. Top. Quantum Electron. **1**, 792 (1995).
[137] A. Taylor, C. Tallman, J. Roberts, C. Lester, T. Gosnell, P. Lee, and G. Kyrala, Opt. Lett. **15**, 39 (1990).
[138] S. Szatzmari, F. P. Schaefer, E. Muller-Horche, and W. Muchenheim, Opt. Commun. **63**, 305 (1987).
[139] B. Bouma, T. Luk, K. Boyer, and C. Rhodes, J. Opt. Soc. Am. B **10**, 1180 (1993).
[140] Y. Nabekawa, K. Kondo, N. Sarukura, K. Sajiki, and S. Watanabe, Opt. Lett. **18**, 1922 (1993).
[141] Y. Nabekawa, K. Sajiki, D. Yoshitomi, K. Kondo, and S. Watanabe, Opt. Lett. **21**, 647 (1996).
[142] S. J. Kane, *Applied Physics* (University of Michigan Press, Ann Arbor, MI, 1996), p. 137.
[143] R. Szipocs, K. Ferencz, C. Spielmann, and F. Krausz, Opt. Lett. **19**, 201 (1994).
[144] M. Wefers and K. Nelson, J. Opt. Soc. Am. B **12**, 1343 (1995).
[145] C. Hillegas, J. Tull, D. Goswami, D. Strickland, and W. Warren, Opt. Lett. **19**, 737 (1994).
[146] J. Sweetser, D. Fittinghoff, and R. Trebino, Opt. Lett. (submitted).
[147] G. Taft, A. Rundquist, H. C. Kapteyn, M. M. Murnane, K. DeLong, R. Trebino, and I. P. Christov, Opt. Lett. **20**, 743 (1995).
[148] Du and *et al.*, Opt. Lett. **20**, 2114 (1995).
[149] W. H. Knox, Appl. Phys. B: Lasers Opt. **B58**, 225 (1994).
[150] W. Warren, H. Rabitz, and M. Dahleh, Science **259**, 1581 (1993).
[151] D. Schumacher, J. Hoogenraad, D. Pinkos, and P. Bucksbaum, Phys. Rev. A **52**, 4719 (1995).
[152] Z. Chang, A. Rundquist, H. Wang, H. C. Kapteyn, and M. M. Murnane, Phys. Rev. Lett. (submitted).